TITLE

Human Cytomegalovirus modifies placental small extracellular vesicle secretion and composition towards a proviral phenotype to enhance infection of fetal recipient cells

AUTHORS

Mathilde Bergamelli [1], Hélène Martin [1], Yann Aubert [1], Jean-Michel Mansuy [2], Marlène Marcellin [3], Odile Burlet-Schiltz [3], Ilse Hurbain [4,5], Graça Raposo [4,5], Jacques Izopet [1,2], Thierry Fournier [6], Alexandra Benchoua [7], Mélinda Bénard [1,8], Marion Groussolles [1,9,10], Géraldine Cartron [11], Yann Tanguy le Gac [11], Nathalie Moinard [12,13], Gisela D'Angelo [4] and Cécile E. Malnou [1]*

* corresponding author

AFFILIATIONS

[1] Institut Toulousain des Maladies Infectieuses et Inflammatoires (Infinity), Université de Toulouse, INSERM, CNRS, UPS, Toulouse, France.

[2] CHU Toulouse, Hôpital Purpan, Laboratoire de Virologie, Toulouse, France.

[3] Institut de Pharmacologie et de Biologie Structurale, IPBS, Université de Toulouse, CNRS, UPS, Toulouse, France.

[4] Institut Curie, CNRS UMR144, Structure et Compartiments Membranaires, Université Paris Sciences et Lettres, Paris, France.

[5] Institut Curie, CNRS UMR144, Plateforme d'imagerie cellulaire et tissulaire (PICT-IBiSA), Université Paris Sciences et Lettres, Paris, France.

[6] Université de Paris, Inserm, UMR-S1139, Physiopathologie & pharmacotoxicologie du placenta humain, microbiote pré & postnatal (3PHM), F-75006 Paris, France.

[7] CECS, I-STEM, AFM, Evry, France.

[8] CHU Toulouse, Hôpital des Enfants, Service de Néonatalogie, Toulouse, France.

[9] CHU Toulouse, Hôpital Paule de Viguier, Service de Diagnostic Prénatal, Toulouse, France.

[10] Equipe SPHERE Epidémiologie et Analyses en Santé Publique: Risques, Maladies chroniques et handicaps, Université de Toulouse, INSERM UMR1027, UPS, Toulouse, France.

[11] CHU Toulouse, Hôpital Paule de Viguier, Service de Gynécologie Obstétrique, Toulouse, France.
[12] Développement Embryonnaire, Fertilité, Environnement (DEFE), INSERM UMR 1203, Université de Toulouse et Université de Montpellier, France.
[13] CECOS, Groupe d'activité de médecine de la reproduction, CHU Toulouse, Hôpital Paule de Viguier, Toulouse, France.

ABSTRACT (179 words)

Although placental small extracellular vesicles (sEVs) are extensively studied in the context of pregnancy, little is known about their role during human cytomegalovirus (hCMV) congenital infection, especially at the beginning of pregnancy. In this study, we examined the consequences of hCMV infection on sEVs production and composition using an immortalized human cytotrophoblast cell line derived from first trimester placenta. By combining complementary approaches of biochemistry, imaging techniques and quantitative proteomic analysis, we showed that hCMV infection increased the yield of sEVs produced by cytotrophoblasts and modified their protein composition towards a proviral phenotype. We further demonstrated that sEVs secreted by hCMV-infected cytotrophoblasts potentiated infection in naive recipient cells of fetal origin, including neural stem cells. Importantly, the enhancement of hCMV infection was also observed with sEVs prepared from either an *ex vivo* model of infected histocultures from early placenta or from the amniotic fluid of patients naturally infected by hCMV at the beginning of pregnancy. Based on these findings, we propose that placental sEVs could be key actors favoring viral dissemination to the fetal brain during hCMV congenital infection.

KEYWORDS

hCMV, congenital infection, extracellular vesicles, placenta, cytotrophoblast, neural stem cells

INTRODUCTION

Human cytomegalovirus (hCMV) belongs to the *Herpesviridae* family and its prevalence is of 50 to 90 % in global human population. Most of the hCMV infections

64 occurring among immunocompetent adults induce an asymptomatic acute replication phase
65 followed by a lifelong persistent latent state. However, hCMV primo-infection, reinfection
66 and/or reactivation may severely compromise the health of immunocompromised people,
67 and is a major issue during pregnancy [1-3]. Indeed, congenital infection by hCMV affects 1%
68 of live births in western countries, making hCMV the most frequently transmitted virus *in*
69 *utero* [3, 4], causing placental and fetal impairments of variable severity. The most severe
70 consequences are observed when transmission occurs during first trimester or in peri-
71 conceptional period [5]. Infection of the placenta itself allows the virus to actively replicate
72 and enable its further access to the fetus [4, 6-10]. The infected placenta can develop a
73 pathology that may lead to miscarriage, premature delivery, *intra* uterine growth
74 retardation or even fetal death [3, 5, 11]. On the other side, the infection of the fetus causes
75 various visceral and central nervous system damage, congenital hCMV infection being the
76 most common cause of brain malformations and deafness of infectious origin [3, 12-15].
77 Despite the extensive research conducted so far, the pathophysiology of hCMV infection
78 remains unclear, especially concerning potential factors which may explain the wide variety
79 of clinical manifestations and their severity [3].
80 In the course of hCMV congenital infection, the placenta is a central key organ, which
81 is the target of viral replication allowing further vertical transmission towards the fetus.
82 Amongst the numerous placental functions, a recently described and extensively studied
83 mode of communication between both maternal and fetal sides consists in the production of
84 placental extracellular vesicles (EVs) [16, 17]. EVs are membranous vesicles secreted by cells
85 in both physiological and pathological situations, which main subtypes can be distinguished
86 depending on their biogenesis and size into small EVs (sEVs) and large EVs (lEVs). They are
87 specifically composed of various molecules such as proteins, lipids and coding and non-
88 coding RNAs [18, 19]. Once released into the extracellular space, EVs can be internalized by
89 other cells, in their immediate environment or within long distances, wherein they exert
90 regulatory roles [20]. For example, there can be uptaken by Natural Killer cells [21, 22] or by
91 primary placental fibroblasts [23]. Although the understanding of the biological relevance of
92 placental EVs *in vivo* remains limited, recent findings highlight their roles in cell-cell
93 communication underlying the feto-placenta-maternal dialogue during pregnancy [24-26].
94 Interestingly, placental EVs content is altered upon gestational diseases such as
95 preeclampsia, preterm birth or gestational diabetes mellitus, and recent literature points

96 towards a putative role of dysregulated placental EVs during pathological pregnancies [25,
97 27-32]. Besides, previous works indicate that term placental EVs may confer an antiviral
98 activity to recipient cells, notably *via* the presence of microRNAs deriving from the C19MC
99 cluster [33-35].

100 Although placental EVs are extensively studied in the context of pregnancy diseases,
101 little is currently known about their role during hCMV congenital infection, especially at the
102 very beginning of pregnancy where most severe sequelae take their origin. A recent study
103 from our team described a dysregulation of the surface expression of placental sEV markers
104 upon hCMV infection in an *ex vivo* model of first trimester placental histoculture, suggesting
105 a putative role for viral dissemination [36]. In the present study, we used immortalized
106 cytotrophoblasts derived from first trimester placenta [37] to comprehensively examine the
107 consequences of hCMV infection on sEVs. We show that hCMV increases the sEV production
108 by cytotrophoblasts and alters their protein content towards a proviral phenotype. Finally,
109 we observe that sEVs secreted by hCMV-infected cytotrophoblasts potentiate infection in
110 naive recipient cells, including neural stem cells. Importantly, this enhancement of hCMV
111 infection is also observed both with sEVs prepared from *ex vivo* early placental histocultures
112 and with sEVs purified from amniotic fluid of patient infected by hCMV during first trimester
113 of pregnancy. Our study provides evidence suggesting that placental sEVs could be key
114 players favoring viral dissemination towards fetal brain during hCMV congenital infection.
115

116 **MATERIALS AND METHODS**

117 **Human ethic approval**

118 The use of neural stem cells (NSCs) from human embryonic stem cells was approved by the
119 French authorities (Agence de la Biomédecine, authorization number SASB0920178S).
120 For the use of human samples and their associated data, the biological resource center
121 Germethèque (BB-0033-00081; declaration: DC-2014-2202; authorization: AC-2015-2350)
122 obtained the written consent from each patient (CPP.2.15.27). For first trimester placenta
123 explants, the steering committee of Germethèque gave its approval for the realization of this
124 study on Feb 5th, 2019. The hosting request made to Germethèque bears the number
125 20190201 and its contract is referenced under the number 19 155C. For amniotic fluid,
126 approval was obtained on July 12th, 2019, the hosting request bears the number 20190606
127 and the contract is referenced under the number DIR-20190823022.

128

129 **Cell lines**

130 MRC5 cells (RD-Biotech), human fetal pulmonary fibroblasts permissive for hCMV, were
131 cultured in Dulbecco's Modified Eagle Medium (DMEM with Glutamax, Gibco) in the
132 presence of 10% fetal bovine serum (FBS, Sigma-Aldrich), 100 U/ml penicillin - 100 µg/ml
133 streptomycin (Gibco) and 100 µg/ml normocin (Invivogen).

134 Extravillous cytotrophoblasts (HIPEC) were obtained from Dr T. Fournier (Inserm, Paris;
135 Transfer agreement n°170448). They were cultured in DMEM / F12 medium (Gibco) at 50/50
136 ratio (v/v), with the same supplementation as MCR5. To purify sEVs from cytotrophoblasts,
137 culture medium was previously depleted from EVs to obtain "Exofree" medium. To this aim,
138 DMEM supplemented with 20 % FBS was ultracentrifuged at 100,000 g for 16 hours at 4 °C
139 (rotor SW32Ti, with maximal acceleration and brake) and filtered at 0.22 µm. Exofree
140 medium was then obtained by a 1:1 dilution with F12 to reach 10 % FBS, with addition of
141 antibiotics as previously described.

142 NSCs were obtained from Dr A. Benchoua (I-Stem, Evry, France). NSC lineage was produced
143 from ES human cells (SA001, I-STEM, UMR861 France) [38] and were maintained in growth
144 medium consisting of DMEM / F12 / Neurobasal medium (Gibco) mixed at a ratio of 1/1/2
145 (v/v/v) in the presence of N2 (50 µL/mL) and B27 without vitamin A supplements (Gibco), 10
146 ng/ml FGF2 (Fibroblast Growth Factor), 10 ng/ml EGF (Epidermal Growth Factor), 20 ng/ml
147 BDNF (Brain-Derived Neurotrophic Factor; all from Peprotech). Beforehand, culture supports
148 were coated by PBS containing poly-L-ornithine (3,3 µg/cm^2; Sigma) then by PBS containing
149 mouse laminin (1 µg/cm^2; Roche), each step followed by extensive washes. Stem character
150 of NSCs was systematically assessed by immunofluorescence against Nestin and SOX2
151 proteins (data not shown).

152 Cell cultures were checked for the absence of mycoplasma (Plasmotest, Invivogen, Toulouse,
153 France).

154

155 **Virus production, titration and infection**

156 The endotheliotropic VHL/E strain of hCMV - a gift from Dr C. Sinzger, University of Ulm,
157 Germany - was used in this study [39]. Viral stocks were obtained upon amplification of the
158 virus on MRC5 cells and concentrated by ultracentrifugation, as already described [14]. Virus
159 titration was realized by indirect immunofluorescence against the Immediate Early (IE)

160 antigen of hCMV, upon infection of MRC5 cells by serial dilutions of the viral stock [14]. In
161 some experiments, virus titration was also performed by qPCR from cell culture
162 supernatants [40].
163 To purify sEVs from infected cells, 4 million cytotrophoblasts were seeded in 150 cm^2 flask,
164 with 6 flasks per condition. 24 h later, cells were infected or not by hCMV at multiplicity of
165 infection (MOI) of 10 (Supplementary Figure 1A). Culture medium was replaced by Exofree
166 medium 24 h post-infection, after having previously ensured that this did not affect the cell
167 growth (Supplementary Figure 1B). Culture supernatants were collected at 48 h and 72 h
168 post-infection, times at which 50-80 % of cells were infected as assessed by IE
169 immunofluorescence (Supplementary Figure 1C). Medium were pooled for each condition
170 (non-infected or infected) and submitted to sEV preparation protocol. Cell number at the
171 end of the experiment was determined by counting upon trypsinization and cell viability
172 evaluated by trypan blue.
173
174 **sEV preparation**
175 Procedures were realized as described previously [36], according to ISEV guidelines [41]. All
176 steps were performed at 4 °C and PBS solution was filtered on a 0.22 µm filter. A preclearing
177 centrifugation of the conditioned medium was carried out for 30 min at 1,200 g to eliminate
178 dead cells and large debris, followed by a second ultracentrifugation for 30 min at 12,000 g
179 (rotor SW32Ti, with maximal acceleration and brake) to eliminate large EVs (principally
180 microvesicles) and the majority of viruses. A last ultracentrifugation was done for 1 hour at
181 100,000 g (Rotor SW32Ti, with maximal acceleration and brake) allowing to pellet sEVs. The
182 pellet was resuspended either in 100 µl PBS or in diluent C (Sigma) for PKH67 staining of the
183 vesicles (Sigma), according to the manufacturer's instructions (5 min incubation; 1:1,000
184 dilution). Pellet was diluted in a solution of 40 % iodixanol in sucrose before
185 ultracentrifugation on a discontinuous iodixanol/sucrose gradient (10 to 40 % iodixanol) with
186 deposition of the sEVs on the bottom of the tube, during 18 h at 100,000 g (rotor SW41Ti,
187 acceleration 5, no brake), to separate sEV from remaining viruses [34, 36, 42]. Six fractions of
188 1.7 ml were collected, fractions 2+3 were pooled and washed in 25 ml PBS. After a last
189 ultracentrifugation for 1 h at 100,000 g (Rotor SW32Ti, with maximal acceleration and
190 brake), the sEV pellet was resuspended in PBS, aliquoted and stored at -80 °C. We submitted

191 all relevant data to the EV-TRACK knowledgebase (EV-TRACK ID: EV210154) and obtained an
192 EV-METRIC score of 100 % for trophoblast and placental explants EVs [43].
193
194 **Nanoparticle tracking analysis (NTA)**
195 sEV preparations were diluted 1:100 in filtered PBS (0.22 µm) and tracked using a NanoSight
196 LM10 (Malvern Panalytical) equipped with a 405 nm laser. Videos were recorded three times
197 for each sample at constant temperature (22 °C) during 60 s and analyzed with NTA
198 Software 2.0 (Malvern instruments Ltd). Data were analyzed with Excel and GraphPad Prism
199 (v8) softwares.
200
201 **Transmission electron microscopy and immunolabeling electron microscopy**
202 Procedures were performed essentially as described [36, 44, 45]. sEV preparations were
203 loaded on copper formvar/carbon coated grids (Ted Pella) and fixed with 2 %
204 paraformaldehyde in 0.1 M phosphate buffer (pH 7.4). For immunolabeling electron
205 microscopy (IEM), immunodetection was carried out with the following primary antibodies:
206 mouse anti-human CD63 (Abcam ab23792), mouse anti-human CD9 or mouse anti-human
207 CD81 (both from Dr E. Rubinstein, Université Paris-Sud, Institut André Lwoff, Villejuif,
208 France). Secondary incubation was performed with a rabbit anti mouse Fc fragment (Dako
209 Agilent Z0412), then grids were incubated with Protein A-Gold 10 nm (Cell Microscopy
210 Center, Department of Cell Biology, Utrecht University). Finally, a second fixation step with 1
211 % glutaraldehyde in PBS was performed and samples were stained with 4 % uranyl acetate in
212 methylcellulose. All samples were observed with a Tecnai Spirit electron microscope (FEI,
213 Eindhoven, The Netherlands), and digital acquisitions were made with a numeric 4k CCD
214 camera (Quemesa, Olympus, Münster, Germany). Images were analysed with iTEM software
215 (EMSIS) and statistical studies were done with GraphPad Prism software (v8).
216
217 **Multiplex bead-based flow cytometry assay**
218 Bead-based multiplex analysis using the MACSPlex Exosome Kit, human (Miltenyi Biotec)
219 were realized on sEV preparations by flow cytometry according to the manufacturer's
220 instructions [46, 47], and as described previously [36]. This allowed the quantification of 39
221 different EV markers, distinguishable by flow cytometry by a specific PE and FITC labeling.
222 The MACSQuant Analyzer 10 flow cytometer (Miltenyi Biotec) was used for analysis. The tool

223 MACSQuantify was used to analyze data (v2.11.1746.19438). GraphPad Prism (v8) software
224 was used to perform statistical analysis of the data.
225
226 **Western blot**
227 sEV samples were lysed in non-reducing conditions in Laemmli buffer, heated for 5 min at 95
228 °C, and loaded on mini protean TGX precast 4-20 % gradient gels (Biorad) in Tris-glycine
229 buffer. Electrophoresis was performed at 110 V for 2 h, then proteins were electro-
230 transferred onto nitrocellulose membranes using the trans-blot turbo transfer system
231 (Biorad). Membranes were blocked with Odyssey blocking buffer (Li-Cor Biosciences) for 1 h,
232 then incubated with different primary antibodies: mouse anti-CD81 (200 ng/ml, Santa-Cruz),
233 mouse anti-CD63 (500 ng/ml, BD Pharmingen), mouse anti-CD9 (100 ng/ml, Millipore),
234 rabbit anti-Tsg101 (1 µg/ml, Abcam), rabbit anti-Alix (1 µg/ml, Abcam), mouse anti-Thy1 (0.5
235 µg/ml, Biolegend), rabbit anti-Tom20 (1/500, Sigma) or goat anti-Calnexin (2 µg/ml, Abcam)
236 overnight at 4 °C in Odyssey blocking buffer, followed by incubation with the secondary
237 antibody IRDye 700 anti-mouse IgG or IRDye 800 anti-rabbit or anti-goat IgG (Li-Cor
238 Biosciences) for 1 h at room temperature. Membranes were washed three times in TBS 0.1
239 % Tween 20 during 10 min after each incubation step and visualized using the Odyssey
240 Infrared Imaging System (LI-COR Biosciences).
241
242 **Quantitative proteomic analysis**
243 *Sample preparation*
244 Protein samples in Laemmli buffer (3 biological replicates of sEVs preparation from non-
245 infected and hCMV-infected cytotrophoblasts cells) were submitted to reduction and
246 alkylation (30 mM DTT and 90 mM iodoacetamide, respectively). Protein samples were
247 digested with trypsin on S-trap Micro devices (Protifi) according to manufacturer's protocol,
248 with the following modifications: precipitation was performed using 545 µl S-Trap buffer and
249 1 µg Trypsin was added per sample for digestion.
250 *NanoLC-MS/MS analysis*
251 Peptides were analyzed by nanoLC-MS/MS using an UltiMate 3000 RSLCnano system
252 coupled to a Q-Exactive-Plus mass spectrometer (Thermo Fisher Scientific, Bremen,
253 Germany). Five µL of each sample were loaded on a C-18 precolumn (300 µm ID x 5 mm,
254 Dionex) in a solvent made of 5 % acetonitrile and 0.05 % TFA and at a flow rate of 20 µL/min.

255 After 5 min of desalting, the precolumn was switched online with the analytical C-18 column
256 (75 µm ID x 15 cm, Reprosil C18) equilibrated in 95 % solvent A (5 % acetonitrile, 0.2 %
257 formic acid) and 5 % solvent B (80 % acetonitrile, 0.2 % formic acid). Peptides were eluted
258 using a 5 to 50 % gradient of solvent B over 105 min at a flow rate of 300 nL/min. The Q-
259 Exactive-Plus was operated in a data-dependent acquisition mode with the XCalibur
260 software. Survey scan MS were acquired in the Orbitrap on the 350-1500 m/z range with the
261 resolution set to a value of 70000. The 10 most intense ions per survey scan were selected
262 for HCD fragmentation. Dynamic exclusion was employed within 30 s to prevent repetitive
263 selection of the same peptide. At least 3 injections were performed for each sample.
264 *Bioinformatics data analysis of mass spectrometry raw files*
265 Raw MS files were processed with the Mascot software for database search and with Proline
266 [48] for label-free quantitative analysis. Data were searched against *Human herpesvirus* 5
267 and Human entries of the UniProtKB protein database (Human betaherpesvirus 5 clone VHL-
268 E-BAC19 and release Uniprot Swiss-Prot February 2018). Carbamidomethylation of cysteines
269 was set as a fixed modification, whereas oxidation of methionine was set as variable
270 modification. Specificity of trypsin/P digestion was set for cleavage after K or R, and two
271 missed trypsin cleavage sites were allowed. The mass tolerance was set to 10 ppm for the
272 precursor and to 20 mmu in tandem MS mode. Minimum peptide length was set to 7 amino
273 acids, and identification results were further validated in Proline by the target decoy
274 approach using a reverse database at both a PSM and protein false-discovery rate of 1%.
275 After mean of replicate injections, the abundance values were log2 transformed and missing
276 values were replaced by random numbers drawn from a normal distribution with a width of
277 0.3 and down shift of 1.8 using the Perseus toolbox (version 1.6.7.0). For statistical analysis,
278 a Student *t*-test (two-tailed *t*-test, equal variances) was then performed on log2 transformed
279 values to analyse differences in protein abundances in all biologic group comparisons.
280 Significance level was set at p = 0.05, and log2 ratios were considered relevant if higher than
281 1 or lower than -1. The mass spectrometry proteomics data have been deposited to the
282 ProteomeXchange Consortium via the PRIDE [49] partner repository with the dataset
283 identifier PXD029146.
284
285 **Functional proteomic data analysis**

286 Volcano plot was established for proteins whose mean abundance exhibited a log2 ratio
287 higher than 1 or lower than -1 and when Student's *t*-test *p*-values were <= 0.05 between the
288 infected and the non-infected conditions. The list of human proteins exhibiting a normalized
289 mean protein abundance log2 ratio > 1 or < -1 between sEVs from non-infected or hCMV-
290 infected samples was used as an input for analysis with QIAGEN Ingenuity Pathway Analysis
291 (IPA) [50]. Results from IPA biological functions and diseases analysis were filtered to
292 retrieve annotations having an absolute activation z-score > 1 and defined by less than 150
293 molecules. The resulting annotations were manually curated to remove redundant
294 annotations sharing identical genes, keeping annotations defined by the greater number of
295 molecules.
296
297 **Flow cytometry analysis**
298 After incubation of cells with PKH67-stained sEVs, cells were washed twice with PBS and
299 trypsinized, before proceeding to flow cytometry analysis. PKH67 positive cells were
300 analyzed on a Macsquant VYB Flow Cytometer (Miltenyi Biotec), by using FCS and FITC
301 fluorescence parameters, and by subtracting cell autofluorescence background. Data were
302 analyzed with FlowJo (BD) and GraphPad Prism (v8) software.
303
304 **Immunofluorescence**
305 Cells were fixed using 4 % PFA (Electron microscopy Sciences) at room temperature for 20
306 min, followed by PBS wash. Permeabilization was then performed with PBS 0,3 % Triton-
307 X100 (Thermofisher scientific) for 10 min at room temperature, followed by 1 h incubation in
308 blocking buffer (PBS with 5 % FBS). Incubation with primary antibodies diluted in blocking
309 buffer was carried out overnight at 4 °C, against hCMV immediate early protein 1 and 2 (1
310 µg/ml; Abcam IE1/IE2 CH160 ab53495), nestin (4 µg/ml; Abcam 10C2 ab 22035), or SOX2
311 (1/500 of stock; Cell Signaling D6D9 #3579). Secondary antibody incubation (Goat anti
312 mouse or rabbit - Alexa-fluor 488 or 594 (2 µg/ml; Thermo Fischer Scientific)) was performed
313 at room temperature for 1 h. For actin staining, Alexa-fluor 568 phalloidin (5 µg/ml; Thermo
314 Fischer Scientific A12380) was incubated on cells overnight at 4°C. DAPI staining (1 µg/ml;
315 Sigma) was performed for 10 min at room temperature. ProLong Gold without DAPI (Thermo
316 Fischer Scientific) was used for coverslip mounting.

317 Widefield acquisitions were realized using Apotome microscope (Zeiss) and confocal
318 acquisitions were made on SP8-STED microscope (Leica). Image processing was performed
319 using ImageJ. GraphPad Prism (v8) software was used to perform data statistical analysis.
320
321 **Placental histoculture**
322 Placental histocultures were carried out as described [36, 51]on first trimester placentas (4
323 placentas; mean = 13.11 ± 0.49 (SEM) weeks of amenorrhea, *i.e.,* 11.11 ± 0.49 weeks of
324 pregnancy; age of the women: mean = 23 ± 1.5 (SEM) year-old), following elective abortion
325 by surgical aspiration at Paule de Viguier Maternity Hospital (Toulouse, France). Briefly,
326 trophoblastic villi were manually dissected in small explants (2-3 mm^3), washed in PBS, and
327 kept overnight in Exofree medium to eliminate the remaining red blood cells. To infect
328 placental explants by hCMV, an overnight incubation of half of the explants was performed
329 upon dissection with 500 µl of pure viral stock (corresponding to around 10^8 focus forming
330 units, ffu) mixed with 500 µl of Exofree medium. Explants were then washed in PBS and
331 deposited nine by nine on gelatin sponges (Gelfoam, Pfizer) in a 6-well plate containing 3 ml
332 of Exofree medium, in at least 6 wells per condition (non-infected *versus* infected).
333 Conditioned medium was collected and renewed with fresh Exofree medium every 3 to 4
334 days for the duration of the culture. At 14 days of culture, total collected medium was
335 pooled for each condition and used to perform sEV preparation as described above.
336 Placental explants were weighed for normalization of resuspension volume and calculation
337 of sEV yield.
338
339 **Amniotic fluid collection**
340 Remaining amniotic fluid (AF) collected during classic patient care was saved for the present
341 study. It was subjected to a 10 min centrifugation at 3000 rpm in order to remove the cells
342 and large debris before its storage at -80 °C. The sEV preparation was carried out according
343 to the procedure described above.
344
345 **RESULTS**
346 **Cytotrophoblast infection by hCMV leads to an increase of sEV secretion**
347 To study the consequences of hCMV infection on placental sEV secretion and
348 composition in early pregnancy, we used an immortalized cell line derived from first

349 trimester extravillous cytotrophoblasts (HIPEC [37, 52]), for which the expression of the
350 cytokeratin 7 specific cytotrophoblastic marker was verified (data not shown). Cell
351 supernatants were collected and pooled upon 48-72 h of infection before sEV preparation.
352 To exclude any possible effect of viral contamination of sEV preparations in further
353 experiments, an infectivity test was systematically carried out at the end of the sEV
354 preparations (Supplementary Figure 1A). When sEV isolated from infected or non-infected
355 cytotrophoblasts were incubated with MRC5 cells, no infection was detected either by
356 immunofluorescence done against IE, nor by RT-qPCR against the viral mRNA encoding UL55
357 protein (Figure 1A). In contrast, cells incubated with hCMV at a MOI of 3 showed active viral
358 replication. Moreover, no structure evoking hCMV viral particle was observed on sEVs
359 isolated from infected cells by TEM (Supplementary Figure 2 and data not shown).
360 Counting of infected cytotrophoblasts at the time of sEV preparation procedure
361 showed a significant decrease of cell number upon hCMV infection compared to non-
362 infected cells (Supplementary Figure 1D) with, however, no overt cell mortality assessed by
363 trypan blue staining (data not shown). Despite the lower cell number upon infection, the
364 quantification of sEVs isolated per cell showed a significant higher yield of production by
365 hCMV-infected cytotrophoblasts compared to non-infected cytotrophoblasts, with an
366 increase of around 40 % upon infection (Figure 1B). However, no difference in either the
367 mean size or the mode size of the sEV preparations was observed upon infection when
368 analyzed by NTA (Figure 1C) and vesicles deriving for both non-infected or infected
369 cytotrophoblasts exhibited the typical structure and shape of sEVs as evidenced by TEM
370 (Figure 1D and Supplementary Figure 2). Relative size distribution was next determined by
371 TEM, by evaluating the relative size of sEV on three independent preparations and for at
372 least 1100 sEV per condition (Figure 1E and F). By using this approach, a significant change in
373 relative size distribution and a global decrease of sEV relative size was observed upon hCMV
374 infection. Indeed, relative size of sEV produced from non-infected cytotrophoblasts was 110
375 nm and decreased to 97 nm for sEV deriving from hCMV-infected cytotrophoblasts.
376
377 **Impact of hCMV infection on canonical sEV markers**
378 To assess the impact of hCMV infection on the expression of sEV canonical markers,
379 different analyses were carried out. By combining western-blotting, multiplex bead-based
380 flow cytometry and immunolabeling electron microscopy, we observed that sEVs

381 preparations expressed specific vesicular markers including CD9, CD81, Alix and Tsg101,
382 without contamination by any endoplasmic reticulum or mitochondrial marker (Figure 2),
383 confirming the quality of the sEV isolation procedure [41]. No drastic differences were
384 observed in their expression between sEVs isolated from non-infected or infected
385 cytotrophoblasts (Figure 2).

386 A multiplex bead-based flow cytometry assay, realized against a panel of proteins
387 [46, 47], indicated that surface proteins expressed by cytotrophoblasts were highly
388 represented on isolated sEVs, like CD24 (a mucin-like glycoprotein expressed by the
389 cytotrophoblasts from the first trimester of pregnancy [53]), CD41b (also known as Integrin
390 alpha 2b, implicated in adhesion and migration of cytotrophoblasts [54]), CD49 (Integrin
391 alpha 5, [55]), CD133 (also called Prominin-1, a pentaspan membrane protein [56]) and
392 SSEA-4 (a stemness marker also expressed by cytotrophoblasts [24]). No significant
393 difference in their surface expression level was observed between sEV isolated from non-
394 infected or hCMV-infected cytotrophoblasts (Figure 2B).

395 In contrast, a striking difference of the expression of the vesicular canonical marker
396 CD63 tetraspanin was evidenced by western-blot. The protein was not detected in whole cell
397 lysates, but was enriched in sEVs isolated specifically from hCMV-infected cytotrophoblasts
398 (Figure 2A). By examining CD63 expression at the level of individual vesicles by IEM, we
399 noticed that this increase was correlated to the presence of a small proportion of sEVs highly
400 positive for CD63 (between 1-5 %, Supplementary Figure 3), while the others remained
401 negative (Figure 2E). By multiplex bead-based flow cytometry assay, no significant difference
402 in CD63 expression could be detected between sEVs prepared from non-infected or infected
403 cytotrophoblasts, certainly due to the low proportion of positive vesicles (Figure 2B). These
404 data revealed that hCMV infection did not globally impact on canonical markers of sEV
405 secreted from cytotrophoblasts, except for CD63 which appeared in a subpopulation of
406 vesicles upon infection.

407

408 **sEVs secreted by infected cytotrophoblasts harbor a proviral protein cargo**

409 To go deeper inside the study of the impact of hCMV infection of trophoblastic cells
410 on sEV cargo, a comprehensive proteomic analysis of sEV composition upon infection was
411 carried out. To this end, equivalent amounts of sEVs prepared from non-infected or hCMV-
412 infected cytotrophoblasts were analyzed by mass spectrometry-based quantitative

413 proteomics for three independent sEV preparations. Each sEV preparation was analyzed with
414 at least three technical replicates, leading to the identification of 1,700 to 1,980 proteins per
415 injection and of 3079 proteins across all samples (3048 human and 31 viral; see
416 Supplementary Table 1 for the list of the proteins identified for the three biological
417 replicates). Among the 3048 human proteins identified, the gProfiler2 R package was able to
418 interrogate 2936 proteins, for which the term "extracellular exosome" (Gene ontology
419 GO:0070062) appeared as the most significantly enriched (false discovery rate
420 (FDR)=1.087859e-^{259}, R package gProfiler2 [57]), with 962 of them (32.8 %) associated with
421 the "extracellular exosome" GO term. Conversely, these 962 proteins constituted 44.1 % of
422 the proteins which define the GO term, and the 94 of the top 100 most frequently identified
423 exosomal proteins, as defined by the Exocarta database
424 (http://exocarta.org/exosome_markers_new), were detected in the sEV preparations.

425 Mass spectrometry-based quantitative proteomics data indicated that 37 proteins,
426 including 25 viral proteins, were significantly over-represented and 15 human proteins
427 under-represented in sEVs secreted by cytotrophoblasts upon hCMV infection, as illustrated
428 in the Volcano plot (Figure 3A). Interestingly, the Thy-1 cellular protein, which has been
429 demonstrated to play an important role to facilitate hCMV entry into cells *via*
430 macropinocytosis [58, 59], was found significantly enriched in sEVs upon infection (Figure 3A
431 and Supplementary Table 1). This was confirmed by western-blot, showing that Thy-1 was
432 detected in sEVs only upon hCMV infection (Supplementary Figure 4A). By using Ingenuity
433 Pathway Analysis (IPA) tool on proteomic data, several biological functions were found to be
434 significantly over- or under-represented in sEVs upon infection (Figure 3B). The highest
435 modulated pathway identified was "autophagy", with several actors showing modified
436 expression in sEVs issued from infected cells, leading to a global autophagy activation
437 pattern (Figure 3C). As EV composition mainly reflects the composition of their secretory
438 cells, this may also reflect the activation of the autophagy pathway induced upon hCMV
439 infection of host cell at the very early times of infection [60-62]. On the other side, two
440 pathways linked to mitochondrial functions (*i.e.,* "consumption of oxygen" and "synthesis of
441 ATP") were found lowered in sEVs prepared from hCMV-infected cells in comparison with
442 non-infected cells (Figure 3B). This also may be the consequence of hCMV-induced
443 mitochondrial dysfunctions [63-66], notably *via* interference with the antiviral Viperin
444 protein, which leads to decreased cellular ATP levels [67].

445 Amongst the proteins identified in sEVs isolated from infected cytotrophoblasts, 31
446 were of viral origin. They are listed in Figure 3D in regards of their biological function,
447 curated from the literature (Supplementary Table 2). They play a role in different aspects of
448 hCMV infection, from viral entry to egress, quiescence, as well as pathogenicity and immune
449 evasion, and are mainly immediate early or late proteins (Supplementary Figure 4B).
450 Interestingly, although sEV preparations were devoid of viral particles as assessed by
451 infectivity assays and TEM, some of the viral proteins found in sEV isolated from hCMV-
452 infected cytotrophoblasts are structural proteins (Figure 3D and Supplementary Table 2), like
453 the envelope proteins gB, gH and gM. Most of the other proteins identified were capsid and
454 tegument proteins that are delivered to host cell upon infection, or proteins immediately
455 expressed after virus entry like IE1 and IE2, which play a role in early transcriptions. Finally,
456 IRS1 and TRS1, which inhibit the establishment of an antiviral state in infected cells, notably
457 by antagonizing the autophagy pathway induced upon hCMV infection [60, 61], were also
458 detected in sEVs isolated from infected cytotrophoblasts. Altogether, analysis of the
459 proteomic data suggested that sEVs secreted by infected cytotrophoblasts may transport a
460 protein cargo with proviral properties, by providing the recipient cells with elements that
461 may facilitate the early steps of a further hCMV infection.
462
463 **sEVs are efficiently uptaken by recipient cells**
464 We next examined whether MRC5 cells may uptake sEVs. To this end, PKH67-stained
465 sEVs prepared from non-infected or infected cytotrophoblasts were incubated with MRC5
466 cells during various times. By performing fluorescence observations of MRC5 cells incubated
467 with PKH67-stained sEVs during 16 h, a vast proportion of cells showed green puncta into
468 their cytoplasm, indicating an important uptake of sEVs (Figure 4A). When performed as
469 soon as 2 h post-incubation, most of the MRC5 cells already showed numerous cytoplasmic
470 puncta, indicating that sEV uptake already occurred at early time points upon sEV incubation
471 with cells, for both sEVs produced by non-infected and infected cytotrophoblasts
472 (Supplementary Figure 5). Moreover, these puncta were visible on the same confocal plan as
473 actin (revealed by phalloidin staining), indicating an intracytoplasmic localization of PKH67
474 fluorescence, and not a simple binding of sEVs to the cell surface (Figure 4A and
475 Supplementary Figures 5B and C).

476 To measure the level of sEV internalization, fluorescence acquisition by recipient cells was
477 then followed by flow cytometry (Figures 4B and C). Percentage of PKH67-positive cells,
478 calculated upon subtraction of cell autofluorescence background, was then calculated
479 depending on duration of incubation with sEVs. As observed in Figures 4B and C, sEV uptake
480 by MRC5 cells was visible as soon as 2 h post-incubation, and reached a maximum of around
481 13 % of positive cells at 16 h, which remained the same until 24 h. However, this percentage
482 may be somewhat underestimated, since subtraction of cell autofluorescence may largely
483 occult an important amount of uptaken sEVs, which fluorescence is faint, given the small size
484 of the vesicles and thus, the small number of PKH67 molecules incorporated. Altogether,
485 these data indicate that the sEVs secreted by cytotrophoblasts are largely uptaken by
486 recipient cells, where they may thereafter exert a biological function.
487
488 **sEVs from hCMV-infected cytotrophoblasts potentialize further infection of recipient**
489 **MRC5 cells**
490 Since proteomic data suggested a proviral activity for sEVs issued from infected
491 cytotrophoblasts, we assessed the ability of sEVs to modulate hCMV infection. As sEV cargo
492 was composed of proteins prone to act on early steps of infection - entry and immediate
493 early transcriptions - we reasoned that any putative action of sEVs should take place
494 immediately after delivery of their content into recipient cells. In this regard, different
495 amounts of sEVs from non-infected or hCMV-infected cytotrophoblasts were deposited on
496 MRC5 cells either concomitantly or 2 h before addition of hCMV (Figure 5A). 24 h later, cells
497 were subjected to an anti-IE immunofluorescence (Figure 5B). When added alone, sEVs
498 prepared from hCMV-infected cells did not lead to any detectable expression of IE in MRC5
499 cells (Figure 5Ba), indicating that they were not contaminated by residual infectious viral
500 particle, as already assessed previously (Figure 1A and Supplementary Figure 2). This also
501 indicated that the detection of IE by immunofluorescence upon infection was due to viral
502 gene expression and not to the presence of IE carried by sEVs, even if it was detected in sEVs
503 secreted by infected cells during proteomic analysis. As observed in Figure 5C, when added
504 simultaneously with hCMV, sEVs did not influence the level of MRC5 cell infection, whatever
505 their origin and quantity, compared to non-treated cells. In contrast, the addition of
506 increasing doses of sEVs prepared from infected cells (sEV hCMV) 2 h before infection led to
507 a potentiation of infection, when compared to cells treated with sEVs prepared from non-

508 infected cells (sEV NI). This increase was significant for the two highest doses of sEVs
509 applied, with a stimulation of infection of around 17 % and 30 % when 50 and 200 sEVs were
510 added per cell, respectively (Figures 5B and D).
511
512 **sEVs from hCMV-infected cytotrophoblasts, placental tissues and amniotic fluids enhance**
513 **infection of human neural stem cells**
514 To examine the potential proviral role of placental sEVs on hCMV transmission
515 towards the fetal brain, we performed similar experiments using human NSCs derived from
516 embryonic stem cells [14, 38]. A significant enhancement of hCMV infection was observed
517 when sEVs prepared from infected cytotrophoblasts were used in comparison to sEVs
518 prepared from non-infected cytotrophoblasts (Figure 6A). A mean increase of 42 % was
519 observed when incubation was done during 24 h, but not with shorter incubation times. This
520 delayed timing of incubation needed for observing a proviral action of sEVs may be due to
521 less efficient sEV fixation and/or uptake mechanisms for NSCs in comparison to MRC5 cells.
522 To get closer to physiological conditions, a model of first trimester placental
523 histocultures was next infected by hCMV and used for sEV isolation. This *ex vivo* model,
524 developed in our team [51, 68], reflects the high complexity of the placental
525 cytoarchitecture. Recent data obtained from this model showed a modification of sEV
526 surface markers upon hCMV infection, which suggested a proviral role of placental sEVs [36].
527 Similar to what was observed with sEVs from cytotrophoblast origin, sEVs produced by
528 infected placental histocultures significantly potentiated hCMV infection of NSCs in
529 comparison to sEVs secreted by non-infected histocultures, with a mean of 48 % of increase
530 upon 24 h of incubation with sEVs (Figure 6B).
531 Finally, the impact of sEVs prepared from amniotic fluid (AF) obtained from naturally
532 infected pregnant women was assessed (Figure 7). Even if AF sEVs originate from various
533 tissues, an important proportion of them have been described to express placental alkaline
534 phosphatase, testifying of their placental origin [69]. Thus, we reasoned that AF sEVs may
535 also be endowed with a proviral activity and facilitate the infection of NSCs by hCMV. AF was
536 collected at third trimester of pregnancy from 3 women, whose clinical data are summarized
537 in Supplementary Table 3. The first one (NP19) had no history of infection or other maternal
538 disease during pregnancy. The second one (NP6) presented a first trimester hCMV
539 seroconversion with her AF negative for hCMV by qPCR and no fetal defects reported by

540 imaging. The third one (NP12) also seroconverted during first trimester of pregnancy but her
541 AF was positive for hCMV by qPCR and the fetus presented major brain lesions. From the AF
542 of these patients, sEVs were prepared and incubated on NCSs during various times before
543 infection by hCMV. NSCs were subjected to an anti-IE immunofluorescence 24 h later to
544 assess their level of infection. A control experiment verifying that no infectious particle was
545 present in sEVs preparations was systematically performed in parallel (data not shown).
546 Compared to the other sources of sEVs used previously (Figure 6), a significant effect of sEVs
547 on viral infection was observed at earlier times of incubation with NSCs but not at 24 h,
548 certainly due to a difference in sEVs uptake efficiency (Figure 7). When incubation was
549 realized simultaneously or 2 h before hCMV infection, level of infection of NSCs incubated
550 with sEVs prepared from the non-infected patient NP19 or NP6 (infected patient but with AF
551 negative for hCMV) remained similar. Remarkably, when sEVs were prepared from NP12, a
552 case of hCMV positive pregnancy with severe impairment of fetal development, a significant
553 increase of infection of around 20 % was observed in comparison to incubation with sEVs
554 from NP6 or NP19, indicating that NP12 sEVs allowed the enhancement of hCMV infection in
555 recipient NSCs. Hence, our data suggest a correlation between the clinical severity of hCMV-
556 complicated pregnancy and the proviral effect of sEVs prepared from patient AF.
557
558 **DISCUSSION**
559 Although the role of placental sEVs during normal and pathological pregnancy is
560 extensively studied [25, 26, 28, 32, 70], the impact and consequences of hCMV infection on
561 placental sEVs are far to be deciphered, in particular at the beginning of pregnancy. We
562 recently described that infection of first trimester *ex vivo* placental histocultures modified
563 sEV surface markers, suggesting a potential proviral role of the sEVs [36]. However, the
564 difficulty of purifying high sEVs amounts from this model hampered the possibility to
565 conduct a study combining exhaustive analysis of sEV composition and biological function. In
566 this work, we used a combination of a cytotrophoblast cell line deriving from first trimester
567 placenta [37], *ex vivo* placental histocultures and patient amniotic fluids to isolate sEVs and
568 examine the impact of hCMV infection on their composition and function.
569 Although a high number of publications describe a role of EVs on pregnancy
570 regulation, the nature of the EVs examined is often not precisely stated, and confusion
571 remains about the subtypes of EVs studied. Here, we decided to focus our study on sEVs,

572 considering the amount of data already available concerning their composition and function
573 [26, 29, 32]. By using the gold-standard method based on differential ultracentrifugation
574 followed by density gradient ultracentrifugation, we were able to isolated sEVs devoid of
575 viral particles in a rigorous manner. These were next further characterized by a combination
576 of complementary approaches and presented the typical features of exosomes in terms of
577 size, structure and presence of canonical markers [41]. Since our work did not focus on their
578 biogenesis pathway, we cannot, however, formally state about their endosomal origin. This
579 is why we used the generic term sEVs along the manuscript, as recommended by the MISEV
580 guidelines. Interestingly, we observed the appearance of a subpopulation of CD63-positive
581 sEVs upon hCMV infection. An enhancement of CD63 expression on sEVs was also recently
582 reported in a study describing a dysregulation of EV biogenesis machinery in a model of
583 hCMV-infected human dermal fibroblasts [71]. Given the low numbers of sEVs positive for
584 CD63 in our model, we have not investigated the underlying molecular mechanism of this
585 CD63 upregulation.

586 Similar to what has been described in the study using dermal fibroblasts [71], we
587 observed that hCMV infection of our cytotrophoblast cell line increased the yield of sEVs
588 production. However, this increase was counterbalanced by a reduced cell growth upon
589 infection. Hence, the global quantity of sEVs harvested from hCMV- or mock-infected cells
590 remained similar between both conditions. As hCMV mainly replicates in discrete foci in
591 placenta *in vivo* [72], it is unlikely that hCMV infection would impact on the global quantity
592 of sEVs secreted by the placenta.

593 Our proteomic study on sEVs revealed the presence of viral proteins in the vesicles
594 secreted from infected cells, notably the envelope proteins gB, gH and gM, as it has already
595 been described in other studies [42, 71, 73]. Additionally, many of the identified viral
596 proteins were capsid and tegument proteins that participate to virus particle assembly and
597 release at the end of the replication cycle. They are usually delivered to host cell upon
598 infection by neo-virions or immediately expressed after viral entry process, where they also
599 play crucial roles. Importantly, IE1 and IE2, which are major viral immediate early genes
600 playing a key role in viral genome expression [74-77], were also present in sEVs produced
601 from infected cells. We also identified pp65, which participates to the transactivation of viral
602 major immediate early genes [78, 79], as well as pp71, which stimulates viral immediate
603 early transcription and inhibits the host innate response by targeting STING [80, 81].

604 Interestingly, except for pp71, most of the viral proteins identified in our study have not
605 been described in the other previous proteomic studies of sEVs secreted from hCMV-
606 infected cells [73]. Conversely, some viral proteins identified by Turner *et al*, such as IR11,
607 IRL12, US14, were not found in our study. To reconcile these differences, it is important to
608 keep in mind that our study focused on sEVs secreted by trophoblastic cells between 24 h to
609 72 h upon infection, *i.e.*, at relatively early time points in replication cycle, when viral
610 particles are only beginning to be released from infected cells. Hence, it is tempting to
611 speculate that sEVs secreted at that early step may prime the neighboring cells for viral
612 dissemination and spread. In contrast, in the study of Turner *et al*, which was realized in
613 MRC5 cells, sEV protein composition was assessed at 5 days post infection, when large
614 amounts of viral particles are released from cells. Their proteomic study showed a protein
615 cargo more prone to serve immuno-evasion functions at a later timing of infection, by
616 expressing for example the viral Fc-gamma receptor homologue IR11/gp34 [73]. Hence, it
617 seems that composition of sEV secreted by hCMV-infected cells evolves with time,
618 depending on their state of infection and the step of hCMV replication cycle.

619 In addition to the viral proteins carried by cytotrophoblast sEVs, composition of sEVs
620 for proteins of cellular origin was also altered upon hCMV infection. By using IPA to analyze
621 biological pathway over-represented in sEVs issued from infected cells, the term
622 "autophagy" was the first represented, likely reflecting the autophagy activation induced by
623 hCMV in host cells at the very early times of infection [60-62]. Importantly, TRS1 and IRS1,
624 two viral proteins described to antagonize autophagy at latter time points of the viral cycle
625 [60, 61], were also carried in sEVs, which may consequently inhibit the induction of
626 autophagy in recipient cells upon sEV uptake. One cellular protein, Thy-1, was also found
627 highly over-represented in sEVs from infected cells. Interestingly Thy-1 plays an important
628 role for favoring hCMV entry into cells by macropinocytosis [58, 59]. Hence, all the elements
629 brought by our proteomic analysis of sEVs indicate that they were prone to facilitate viral
630 infection of recipient cells, while inhibiting innate antiviral cellular responses.

631 By examining the function of sEVs isolated from non-infected or hCMV-infected
632 cytotrophoblasts, we observed that sEVs secreted by infected cells enhanced further hCMV
633 infection of MRC5 cells. Such proviral properties of sEVs produced by infected cells have
634 already been described for other *Herpesviridae* [82, 83] and very recently for hCMV [71] -
635 although not in a placental context - and confirm a general role of sEVs in modulating viral

636 transmission for many viral families [84-86]. Since placental sEVs are found both in maternal
637 and fetal sides at high quantities as soon as the early beginning of pregnancy [87, 88], we
638 hypothesized that they may facilitate hCMV dissemination not only in the placental tissues
639 but also towards the fetus, notably in the fetal brain, by enhancing hCMV infectivity in fetal
640 neural cells. Indeed, we observed that sEVs prepared from an infected trophoblast cell line
641 or first trimester placental explants enhanced hCMV infection of human NSCs. Finally, our
642 observations were confirmed using clinical samples. Strikingly, a significant enhancement of
643 infection was observed with sEVs isolated from the amniotic fluid of an infected woman
644 (with amniotic fluid positive for hCMV) whose fetus showed severe neurodevelopmental
645 impairments, in contrast to sEVs isolated from the amniotic fluid of a non-infected pregnant
646 woman, or an infected woman (with amniotic fluid negative for hCMV) whose fetus showed
647 no detectable developmental defects. Hence, placental sEVs seem to be key players of hCMV
648 dissemination towards the fetus during congenital infection and may be one of the missing
649 links explaining the variety and severity of sequelae observed during viral congenital
650 infection.
651
652 **REFERENCES**

653 1. Lanzieri, T.M., et al., *Seroprevalence of cytomegalovirus among children 1 to 5 years*
654 *of age in the United States from the National Health and Nutrition Examination*
655 *Survey of 2011 to 2012.* Clin Vaccine Immunol, 2015. **22**(2): p. 245-7.
656 2. Cannon, M.J., D.S. Schmid, and T.B. Hyde, *Review of cytomegalovirus seroprevalence*
657 *and demographic characteristics associated with infection.* Rev Med Virol, 2010.
658 **20**(4): p. 202-13.
659 3. Leruez-Ville, M., et al., *Cytomegalovirus infection during pregnancy: state of the*
660 *science.* Am J Obstet Gynecol, 2020. **223**(3): p. 330-349.
661 4. Pereira, L., et al., *HCMV persistence in the population: potential transplacental*
662 *transmission*, in *Human Herpesviruses: Biology, Therapy, and Immunoprophylaxis*, A.
663 Arvin, et al., Editors. 2007: Cambridge.
664 5. Pereira, L., et al., *Congenital cytomegalovirus infection undermines early*
665 *development and functions of the human placenta.* Placenta, 2017. **59 Suppl 1**: p. S8-
666 S16.

667 6. Fisher, S., et al., *Human cytomegalovirus infection of placental cytotrophoblasts in*
668 *vitro and in utero: implications for transmission and pathogenesis.* J Virol, 2000.
669 **74**(15): p. 6808-20.
670 7. Pereira, L., et al., *Insights into viral transmission at the uterine-placental interface.*
671 Trends Microbiol, 2005. **13**(4): p. 164-74.
672 8. Tabata, T., et al., *Cytotrophoblasts infected with a pathogenic human*
673 *cytomegalovirus strain dysregulate cell-matrix and cell-cell adhesion molecules: a*
674 *quantitative analysis.* Placenta, 2007. **28**(5-6): p. 527-37.
675 9. Tabata, T., et al., *Cytomegalovirus impairs cytotrophoblast-induced*
676 *lymphangiogenesis and vascular remodeling in an in vivo human placentation model.*
677 Am J Pathol, 2012. **181**(5): p. 1540-59.
678 10. Tabata, T., et al., *Persistent Cytomegalovirus Infection in Amniotic Membranes of the*
679 *Human Placenta.* Am J Pathol, 2016. **186**(11): p. 2970-2986.
680 11. Pereira, L., et al., *Intrauterine growth restriction caused by underlying congenital*
681 *cytomegalovirus infection.* J Infect Dis, 2014. **209**(10): p. 1573-84.
682 12. Leruez-Ville, M. and Y. Ville, *Fetal cytomegalovirus infection.* Best Pract Res Clin
683 Obstet Gynaecol, 2017. **38**: p. 97-107.
684 13. Picone, O., et al., *Detailed in utero ultrasound description of 30 cases of congenital*
685 *cytomegalovirus infection.* Prenat Diagn, 2014. **34**(6): p. 518-24.
686 14. Rolland, M., et al., *PPARgamma Is Activated during Congenital Cytomegalovirus*
687 *Infection and Inhibits Neuronogenesis from Human Neural Stem Cells.* PLoS Pathog,
688 2016. **12**(4): p. e1005547.
689 15. Rolland, M., et al., *Human cytomegalovirus infection is associated with increased*
690 *expression of the lissencephaly gene PAFAH1B1 encoding LIS1 in neural stem cells and*
691 *congenitally infected brains.* J Pathol, 2021. **254**(1): p. 92-102.
692 16. Sarker, S., et al., *Placenta-derived exosomes continuously increase in maternal*
693 *circulation over the first trimester of pregnancy.* J Transl Med, 2014. **12**: p. 204.
694 17. Luo, S.S., et al., *Human villous trophoblasts express and secrete placenta-specific*
695 *microRNAs into maternal circulation via exosomes.* Biol Reprod, 2009. **81**(4): p. 717-
696 29.

697 18. Colombo, M., G. Raposo, and C. Thery, *Biogenesis, secretion, and intercellular*
698 *interactions of exosomes and other extracellular vesicles.* Annu Rev Cell Dev Biol,
699 2014. **30**: p. 255-89.
700 19. van Niel, G., G. D'Angelo, and G. Raposo, *Shedding light on the cell biology of*
701 *extracellular vesicles.* Nat Rev Mol Cell Biol, 2018. **19**(4): p. 213-228.
702 20. Kalluri, R. and V.S. LeBleu, *The biology, function, and biomedical applications of*
703 *exosomes.* Science, 2020. **367**(6478).
704 21. Ishida, Y., et al., *Maternal peripheral blood natural killer cells incorporate placenta-*
705 *associated microRNAs during pregnancy.* Int J Mol Med, 2015. **35**(6): p. 1511-24.
706 22. Chaiwangyen, W., et al., *MiR-519d-3p in Trophoblastic Cells: Effects, Targets and*
707 *Transfer to Allogeneic Immune Cells via Extracellular Vesicles.* Int J Mol Sci, 2020.
708 **21**(10).
709 23. Li, H., et al., *Internalization of trophoblastic small extracellular vesicles and detection*
710 *of their miRNA cargo in P-bodies.* J Extracell Vesicles, 2020. **9**(1): p. 1812261.
711 24. Salomon, C., et al., *Extravillous trophoblast cells-derived exosomes promote vascular*
712 *smooth muscle cell migration.* Front Pharmacol, 2014. **5**: p. 175.
713 25. Malnou, E.C., et al., *Imprinted MicroRNA Gene Clusters in the Evolution,*
714 *Development, and Functions of Mammalian Placenta.* Front Genet, 2019. **9**: p. 706.
715 26. Sadovsky, Y., et al., *Placental small extracellular vesicles: Current questions and*
716 *investigative opportunities.* Placenta, 2020. **102**: p. 34-38.
717 27. Chiarello, D.I., et al., *Foetoplacental communication via extracellular vesicles in*
718 *normal pregnancy and preeclampsia.* Mol Aspects Med, 2018. **60**: p. 69-80.
719 28. Mitchell, M.D., et al., *Placental exosomes in normal and complicated pregnancy.* Am J
720 Obstet Gynecol, 2015. **213**(4 Suppl): p. S173-81.
721 29. Salomon, C. and G.E. Rice, *Role of Exosomes in Placental Homeostasis and Pregnancy*
722 *Disorders.* Prog Mol Biol Transl Sci, 2017. **145**: p. 163-179.
723 30. Salomon, C., et al., *Exosomal signaling during hypoxia mediates microvascular*
724 *endothelial cell migration and vasculogenesis.* PLoS One, 2013. **8**(7): p. e68451.
725 31. Salomon, C., et al., *Gestational Diabetes Mellitus Is Associated With Changes in the*
726 *Concentration and Bioactivity of Placenta-Derived Exosomes in Maternal Circulation*
727 *Across Gestation.* Diabetes, 2016. **65**(3): p. 598-609.

728 32. Jin, J. and R. Menon, *Placental exosomes: A proxy to understand pregnancy*
729 *complications.* Am J Reprod Immunol, 2018. **79**(5): p. e12788.
730 33. Delorme-Axford, E., et al., *Human placental trophoblasts confer viral resistance to*
731 *recipient cells.* Proc Natl Acad Sci U S A, 2013. **110**(29): p. 12048-53.
732 34. Ouyang, Y., et al., *Isolation of human trophoblastic extracellular vesicles and*
733 *characterization of their cargo and antiviral activity.* Placenta, 2016. **47**: p. 86-95.
734 35. Bayer, A., et al., *Chromosome 19 microRNAs exert antiviral activity independent from*
735 *type III interferon signaling.* Placenta, 2018. **61**: p. 33-38.
736 36. Bergamelli, M., et al., *Human Cytomegalovirus Infection Changes the Pattern of*
737 *Surface Markers of Small Extracellular Vesicles Isolated From First Trimester Placental*
738 *Long-Term Histocultures.* Front Cell Dev Biol, 2021. **9**: p. 689122.
739 37. Pavan, L., et al., *Human invasive trophoblasts transformed with simian virus 40*
740 *provide a new tool to study the role of PPARgamma in cell invasion process.*
741 Carcinogenesis, 2003. **24**(8): p. 1325-36.
742 38. Boissart, C., et al., *miR-125 potentiates early neural specification of human embryonic*
743 *stem cells.* Development, 2012. **139**(7): p. 1247-57.
744 39. Stegmann, C., et al., *The N Terminus of Human Cytomegalovirus Glycoprotein O Is*
745 *Important for Binding to the Cellular Receptor PDGFRalpha.* J Virol, 2019. **93**(11).
746 40. Mengelle, C., et al., *Performance of a completely automated system for monitoring*
747 *CMV DNA in plasma.* J Clin Virol, 2016. **79**: p. 25-31.
748 41. Thery, C., et al., *Minimal information for studies of extracellular vesicles 2018*
749 *(MISEV2018): a position statement of the International Society for Extracellular*
750 *Vesicles and update of the MISEV2014 guidelines.* J Extracell Vesicles, 2018. **7**(1): p.
751 1535750.
752 42. Zicari, S., et al., *Human cytomegalovirus-infected cells release extracellular vesicles*
753 *that carry viral surface proteins.* Virology, 2018. **524**: p. 97-105.
754 43. Consortium, E.-T., et al., *EV-TRACK: transparent reporting and centralizing knowledge*
755 *in extracellular vesicle research.* Nat Methods, 2017. **14**(3): p. 228-232.
756 44. Hurbain, I., et al., *Analyzing Lysosome-Related Organelles by Electron Microscopy.*
757 Methods Mol Biol, 2017. **1594**: p. 43-71.
758 45. Raposo, G., et al., *B lymphocytes secrete antigen-presenting vesicles.* J Exp Med,
759 1996. **183**(3): p. 1161-72.

760 46. Koliha, N., et al., *A novel multiplex bead-based platform highlights the diversity of*
761 *extracellular vesicles.* J Extracell Vesicles, 2016. **5**: p. 29975.
762 47. Wiklander, O.P.B., et al., *Systematic Methodological Evaluation of a Multiplex Bead-*
763 *Based Flow Cytometry Assay for Detection of Extracellular Vesicle Surface Signatures.*
764 Front Immunol, 2018. **9**: p. 1326.
765 48. Bouyssie, D., et al., *Proline: an efficient and user-friendly software suite for large-*
766 *scale proteomics.* Bioinformatics, 2020. **36**(10): p. 3148-3155.
767 49. Perez-Riverol, Y., et al., *The PRIDE database and related tools and resources in 2019:*
768 *improving support for quantification data.* Nucleic Acids Res, 2019. **47**(D1): p. D442-
769 D450.
770 50. Thomas, S. and D. Bonchev, *A survey of current software for network analysis in*
771 *molecular biology.* Hum Genomics, 2010. **4**(5): p. 353-60.
772 51. Lopez, H., et al., *Novel model of placental tissue explants infected by cytomegalovirus*
773 *reveals different permissiveness in early and term placentae and inhibition of*
774 *indoleamine 2,3-dioxygenase activity.* Placenta, 2011. **32**(7): p. 522-30.
775 52. Rauwel, B., et al., *Activation of peroxisome proliferator-activated receptor gamma by*
776 *human cytomegalovirus for de novo replication impairs migration and invasiveness of*
777 *cytotrophoblasts from early placentas.* J Virol, 2010. **84**(6): p. 2946-54.
778 53. Sammar, M., et al., *Expression of CD24 and Siglec-10 in first trimester placenta:*
779 *implications for immune tolerance at the fetal-maternal interface.* Histochem Cell
780 Biol, 2017. **147**(5): p. 565-574.
781 54. Rout, U.K., et al., *Alpha5beta1, alphaVbeta3 and the platelet-associated integrin*
782 *alphaIIbbeta3 coordinately regulate adhesion and migration of differentiating mouse*
783 *trophoblast cells.* Dev Biol, 2004. **268**(1): p. 135-51.
784 55. Lee, C.Q., et al., *What Is Trophoblast? A Combination of Criteria Define Human First-*
785 *Trimester Trophoblast.* Stem Cell Reports, 2016. **6**(2): p. 257-72.
786 56. Potgens, A.J., et al., *Human trophoblast contains an intracellular protein reactive with*
787 *an antibody against CD133--a novel marker for trophoblast.* Placenta, 2001. **22**(7): p.
788 639-45.
789 57. Raudvere, U., et al., *g:Profiler: a web server for functional enrichment analysis and*
790 *conversions of gene lists (2019 update).* Nucleic Acids Res, 2019. **47**(W1): p. W191-
791 W198.

792 58. Li, Q., E. Fischer, and J.I. Cohen, *Cell Surface THY-1 Contributes to Human*
793 *Cytomegalovirus Entry via a Macropinocytosis-Like Process.* J Virol, 2016. **90**(21): p.
794 9766-9781.
795 59. Li, Q., et al., *THY-1 Cell Surface Antigen (CD90) Has an Important Role in the Initial*
796 *Stage of Human Cytomegalovirus Infection.* PLoS Pathog, 2015. **11**(7): p. e1004999.
797 60. Chaumorcel, M., et al., *The human cytomegalovirus protein TRS1 inhibits autophagy*
798 *via its interaction with Beclin 1.* J Virol, 2012. **86**(5): p. 2571-84.
799 61. Mouna, L., et al., *Analysis of the role of autophagy inhibition by two complementary*
800 *human cytomegalovirus BECN1/Beclin 1-binding proteins.* Autophagy, 2016. **12**(2): p.
801 327-42.
802 62. Taisne, C., et al., *Human cytomegalovirus hijacks the autophagic machinery and LC3*
803 *homologs in order to optimize cytoplasmic envelopment of mature infectious*
804 *particles.* Sci Rep, 2019. **9**(1): p. 4560.
805 63. Karniely, S., et al., *Human Cytomegalovirus Infection Upregulates the Mitochondrial*
806 *Transcription and Translation Machineries.* mBio, 2016. **7**(2): p. e00029.
807 64. Federspiel, J.D., et al., *Mitochondria and Peroxisome Remodeling across*
808 *Cytomegalovirus Infection Time Viewed through the Lens of Inter-ViSTA.* Cell Rep,
809 2020. **32**(4): p. 107943.
810 65. Combs, J.A., et al., *Human Cytomegalovirus Alters Host Cell Mitochondrial Function*
811 *during Acute Infection.* J Virol, 2020. **94**(2).
812 66. Monk, C.H. and K.J. Zwezdaryk, *Host Mitochondrial Requirements of Cytomegalovirus*
813 *Replication.* Curr Clin Microbiol Rep, 2020. **7**(4): p. 115-123.
814 67. Seo, J.Y., et al., *Human cytomegalovirus directly induces the antiviral protein viperin*
815 *to enhance infectivity.* Science, 2011. **332**(6033): p. 1093-7.
816 68. Benard, M., et al., *Human cytomegalovirus infection induces leukotriene B4 and 5-*
817 *lipoxygenase expression in human placentae and umbilical vein endothelial cells.*
818 Placenta, 2014. **35**(6): p. 345-50.
819 69. Dixon, C.L., et al., *Amniotic Fluid Exosome Proteomic Profile Exhibits Unique Pathways*
820 *of Term and Preterm Labor.* Endocrinology, 2018. **159**(5): p. 2229-2240.
821 70. Adam, S., et al., *Review: Fetal-maternal communication via extracellular vesicles -*
822 *Implications for complications of pregnancies.* Placenta, 2017. **54**: p. 83-88.

823 71. Streck, N.T., et al., *Human Cytomegalovirus Utilizes Extracellular Vesicles To Enhance*
824 *Virus Spread.* J Virol, 2020. **94**(16).
825 72. Uenaka, M., et al., *Histopathological analysis of placentas with congenital*
826 *cytomegalovirus infection.* Placenta, 2019. **75**: p. 62-67.
827 73. Turner, D.L., et al., *The host exosome pathway underpins biogenesis of the human*
828 *cytomegalovirus virion.* Elife, 2020. **9**.
829 74. Mocarski, E.S., et al., *A deletion mutant in the human cytomegalovirus gene encoding*
830 *IE1(491aa) is replication defective due to a failure in autoregulation.* Proc Natl Acad
831 Sci U S A, 1996. **93**(21): p. 11321-6.
832 75. Ahn, J.H. and G.S. Hayward, *The major immediate-early proteins IE1 and IE2 of*
833 *human cytomegalovirus colocalize with and disrupt PML-associated nuclear bodies at*
834 *very early times in infected permissive cells.* J Virol, 1997. **71**(6): p. 4599-613.
835 76. Nevels, M., C. Paulus, and T. Shenk, *Human cytomegalovirus immediate-early 1*
836 *protein facilitates viral replication by antagonizing histone deacetylation.* Proc Natl
837 Acad Sci U S A, 2004. **101**(49): p. 17234-9.
838 77. Wiebusch, L. and C. Hagemeier, *Human cytomegalovirus 86-kilodalton IE2 protein*
839 *blocks cell cycle progression in G(1).* J Virol, 1999. **73**(11): p. 9274-83.
840 78. Cristea, I.M., et al., *Human cytomegalovirus pUL83 stimulates activity of the viral*
841 *immediate-early promoter through its interaction with the cellular IFI16 protein.* J
842 Virol, 2010. **84**(15): p. 7803-14.
843 79. Arcangeletti, M.C., et al., *Cell-cycle-dependent localization of human cytomegalovirus*
844 *UL83 phosphoprotein in the nucleolus and modulation of viral gene expression in*
845 *human embryo fibroblasts in vitro.* J Cell Biochem, 2011. **112**(1): p. 307-17.
846 80. Lukashchuk, V., et al., *Human cytomegalovirus protein pp71 displaces the chromatin-*
847 *associated factor ATRX from nuclear domain 10 at early stages of infection.* J Virol,
848 2008. **82**(24): p. 12543-54.
849 81. Fu, Y.Z., et al., *Human Cytomegalovirus Tegument Protein UL82 Inhibits STING-*
850 *Mediated Signaling to Evade Antiviral Immunity.* Cell Host Microbe, 2017. **21**(2): p.
851 231-243.
852 82. Bello-Morales, R. and J.A. Lopez-Guerrero, *Extracellular Vesicles in Herpes Viral*
853 *Spread and Immune Evasion.* Front Microbiol, 2018. **9**: p. 2572.

854 83. Cone, A.S., S.B. York, and D.G. Meckes, Jr., *Extracellular Vesicles in Epstein-Barr Virus*
855 *Pathogenesis.* Curr Clin Microbiol Rep, 2019. **6**(3): p. 121-131.
856 84. Lenassi, M., et al., *HIV Nef is secreted in exosomes and triggers apoptosis in*
857 *bystander CD4+ T cells.* Traffic, 2010. **11**(1): p. 110-22.
858 85. Chapuy-Regaud, S., et al., *Characterization of the lipid envelope of exosome*
859 *encapsulated HEV particles protected from the immune response.* Biochimie, 2017.
860 **141**: p. 70-79.
861 86. Grunvogel, O., et al., *Secretion of Hepatitis C Virus Replication Intermediates Reduces*
862 *Activation of Toll-Like Receptor 3 in Hepatocytes.* Gastroenterology, 2018. **154**(8): p.
863 2237-2251 e16.
864 87. Liu, H., et al., *Estimation of the burden of human placental micro- and nano-vesicles*
865 *extruded into the maternal blood from 8 to 12 weeks of gestation.* Placenta, 2018. **72-**
866 **73**: p. 41-47.
867 88. Miranda, J., et al., *Placental exosomes profile in maternal and fetal circulation in*
868 *intrauterine growth restriction - Liquid biopsies to monitoring fetal growth.* Placenta,
869 2018. **64**: p. 34-43.
870

871 **FUNDING**

872 This project has received financial support from the French Biomedicine Agency,
873 institutional grants from Inserm, CNRS and Toulouse 3 University. This project is part of the
874 doctorate thesis of Mathilde Bergamelli, who was funded by the Ministry of Education and
875 Research (MESR). The TEM experiments were performed on PICT-IBiSA, Institut Curie, Paris,
876 member of the France-BioImaging national research infrastructure, and were supported by
877 the French National Research Agency through the "Investments for the Future" program
878 (France-BioImaging, ANR-11-INSB-04), supported by the CelTisPhyBio Labex (N° ANR-11-
879 LB0038) part of the IDEX PSL (N°ANR-10-IDEX-0001-02 PSL). The proteomic part of this
880 project was supported in part by the Région Occitanie, European funds (Fonds Européens de
881 Développement Régional, FEDER), Toulouse Métropole, and by the French Ministry of
882 Research with the Investissement d'Avenir Infrastructures Nationales en Biologie et Santé
883 program (ProFI, Proteomics French Infrastructure project, ANR-10-INBS-08).
884

885 **CONFLICTS OF INTEREST**

886 The authors declare that the research was conducted in the absence of any
887 commercial or financial relationships that could be construed as a potential conflict of
888 interest.
889
890 **AUTHOR'S CONTRIBUTION**
891 MBer and HM designed and performed most experiments and analyzed data. JMM
892 and JI were in charge of the viral titrations. MM, OBS and YA performed the proteomic
893 experiments and data analysis. MBén, MG, GC and YTLG collected the clinical samples and
894 data. NM from Germethèque was in charge of the ethical issues and received women
895 authorizations. IH, GDA and GR supervised the electron microscopy experiments and data
896 analysis. TF and AB generated the HIPECs and NSCs respectively, and gave scientific expertise
897 concerning their culture. CEM got grants for this study, conceived and designed the study,
898 analyzed data and wrote the paper, with the help of MBer, YA and OBS. All authors provided
899 critical feedback and helped shape the research, analysis and manuscript.
900
901 **ACKNOWLEDGMENTS**
902 We greatly thank C. Chouquet, B. Rauwel, M. Mouysset, L. Battut, C. Mengelle, F.
903 Chauvrier, P. Verdy, N. Kopf, as well as the whole ViNeDys team, for their technical
904 assistance and their numerous advice and discussions which allowed the progress of this
905 work. We thank also AL. Iscache, V. Duplan-Eche and F. L'Faqihi-Olive, from the cytometry
906 facility of Infinity, as well as S. Allart and D. Daviaud, from the imaging facility of Infinity, and
907 finally the GeT technical service of Infinity. We thank the medical and paramedical staff of
908 the gynecology unit at Paule de Viguier Hospital, the patients who agreed to participate in
909 the study, as well as L. Bujan and M. Aubry, from the Germethèque. We finally warmly thank
910 E. Haanappel from the Institute of Pharmacology and Structural Biology, who granting us
911 access to the Nanosight device, and Audrey Esclatine and Daniel Gonzalez-Dunia for critical
912 reading of the manuscript and insightful comments.
913
914 **FIGURE LEGENDS**
915 **Figure 1: Impact of hCMV on trophoblastic cells sEV production, size and ultrastructure.** A)
916 Immunofluorescence realized against hCMV Immediate Early (IE) antigen in non-treated
917 MRC5 cells (panel a), or upon incubation during 24 h with either hCMV at MOI 3 (panel b),

918 sEVs isolated from non-infected (panel c) or from hCMV-infected cytotrophoblasts (panel d).
919 Magnification = 20 x. Blue (upper panel): DAPI; red (lower panel): IE. Below images are
920 indicated the results of RT-qPCR realized against hCMV UL55 mRNAs on RNA extracted from
921 MRC5 cells at 48 h post-incubation with hCMV or sEV preparations (+: amplification; -: no
922 amplification). Data are representative for at least three independent experiments. B) Yield
923 of sEV recovered upon sEV preparation from non-infected (NI) or infected (hCMV)
924 cytotrophoblasts, calculated upon NTA experiments. *, p = 0.0464 by paired t-test for 7
925 independent experiments. C) Comparison of mean size (left histogram) and mode size (right
926 histogram) between sEVs prepared from non-infected (NI) or infected (hCMV)
927 cytotrophoblasts, calculated upon NTA experiments. Histograms show the mean ± SEM of
928 three independent experiments. ns: non-significant by Mann Whitney test. D) Electron
929 microscopy images of sEV (indicated by an arrow) prepared from non-infected (NI) or
930 infected (hCMV) cytotrophoblasts. Magnification = 26000 X. Scale bar = 100 nm. Images are
931 representative of at least three independent experiments. E) Distribution analysis of sEV
932 relative size measured from MET pictures, for sEV isolated from either non-infected (white
933 bars) or infected cytotrophoblasts (grey bars). Each bar of the histogram represents the
934 mean ± SEM of the number of sEVs per bin (bin width = 20 nm) for three independent
935 experiments. ****, p <0.0001 by Chi-square test. F) Relative size of individual sEVs,
936 measured from MET pictures for three independent experiments, was reported on graph, as
937 well as the mean ± SEM. Total sEV count was 1165 for NI and 1351 for hCMV sEVs. ****, p
938 <0.0001 by Mann-Whitney test.
939
940 **Figure 2: Impact of hCMV infection of trophoblastic cells on sEV canonical markers.** A)
941 Western-blot realized on either whole cell lysates (left wells) or purified sEVs (right wells),
942 from non-infected (NI) or infected (hCMV) cytotrophoblasts. Proteins of interest and their
943 corresponding molecular weight are indicated on the right of the Figure, with a smear for
944 CD63 due to the non-reducing conditions of the western blot, which preserve its rich
945 glycosylated pattern. B) Surface expression level of different proteins found on sEV isolated
946 from non-infected (NI) or infected (hCMV) cytotrophoblasts, determined with the multiplex
947 flow cytometry MACSPlex exosome kit assay. The heat-map represents the mean of 3
948 independent experiments, for different sEV markers indicated on the left column. Blue
949 intensity is proportional to the level of expression calculated in Median Fluorescence

950 Intensity, indicated on the right of the heat-map. ns, non-significant by two-way ANOVA. C-
951 E) TEM observation of sEV - isolated from non-infected (NI) or infected (hCMV)
952 cytotrophoblasts - which were immunogold-labelled for CD9 (C), CD81 (D) or CD63 (E), and
953 revealed with Protein A-gold particle of 10 nm diameter. Scale bar = 100 nm. Magnification =
954 26000 X. In E) only positive vesicles, representing around 1-5 % of sEVs isolated upon
955 infection, are shown, the other being negative (see Supplementary Figure 3 for wide field
956 image).
957
958 **Figure 3: Proteomic analysis of sEV composition upon infection of trophoblastic cells by**
959 **hCMV.** A) Volcano-plot representing differences in normalized mean protein abundance in
960 sEVs hCMV *versus* sEVs NI. Human and viral proteins exhibiting significant differences
961 between the two conditions are represented by circles and triangles, respectively (Student
962 T-test *p*-value <=0.05 and log2 ratio >=1 or <=-1). Red: over- represented proteins; Blue:
963 under- represented proteins. B) Dot plot representation of the top diseases and biological
964 functions associated with human proteins exhibiting an absolute normalized mean
965 abundance log2 ratio greater than 1 or lower than -1, in sEVs hCMV *versus* sEVs NI. Top
966 diseases and biological functions associated with changes in the protein content of sEVs
967 upon hCMV-infection were identified using QIAGEN Ingenuity Pathway Analysis (IPA). Size of
968 the circles depends on the number of the proteins identified in the corresponding pathway;
969 level of blue intensity depends on the *p*-value. C) Human proteins associated with the
970 predicted increased activation state of autophagy pathway as determined by IPA. D)
971 Heatmap representation of the biological functions associated with hCMV viral proteins
972 expressed in sEVs hCMV.
973
974 **Figure 4: Internalization of sEVs isolated from non-infected cytotrophoblasts in fetal MRC5**
975 **cells.** A) Confocal images of fluorescence microscopy carried out on MRC5 cells after 16h
976 incubation with PKH67-labelled sEVs. Blue: DAPI; Red: Phalloidin; Green: PKH67. Scale bar:
977 100 µm. Magnification = 63 X. B) Histogram representing the percentage of PKH67 positive
978 cells along time, upon incubation of MRC5 cells with sEVs. Bars represent the mean ± SEM of
979 three independent experiments. C) Monitoring of PKH67-labeled sEVs internalization by
980 MRC5 cells by flow cytometry. Dot plots represent MRC5 cell fluorescence upon incubation
981 with PKH67-stained sEVs (200 sEVs/cell) for cells that have not been incubated with sEVs

982 (NT, non-treated), or upon 2 h or 16 h of incubation. X-axis: PKH-67 fluorescence intensity; Y-
983 axis: FSC. Gate indicates cells positive for PKH67.
984
985 **Figure 5: Effect of cytotrophoblast sEVs on MRC5 cell permissiveness for hCMV.** A)
986 experimental procedure (NT=non-treated). B) Immunofluorescence performed on MRC5
987 cells against IE viral antigen (blue: DAPI; red: IE). a- Non-infected control cells upon 24 h
988 incubation with sEVs isolated from hCMV-infected cytotrophoblasts. B,c,d- MRC5 cells were
989 either non-treated (b- NT) or incubated during 2 h with sEVs prepared from non-infected (c-
990 sEV NI) or infected cytotrophoblasts (d- sEV hCMV) with 50 sEV per cell, then infected during
991 24 h with hCMV at a MOI of 0.5 before proceeding to immunofluorescence. Scale bar: 200
992 µm. C-D) MRC5 cells were incubated with sEVs prepared from non-infected (sEV NI) or
993 hCMV-infected (sEV hCMV) cytotrophoblasts and infected by hCMV at a MOI of 0.5,
994 concomitantly (C) or 2 h after sEV incubation (D). Three increasing doses of sEVs were used
995 in these experiments (20, 50 or 200 sEV per cell, from left to right). 24 h later, expression of
996 IE antigen was assessed by immunofluorescence. Quantification of the percentage of IE
997 positive cells was carried out and normalized by the percentage of cells infected by hCMV
998 without any sEV (NT). Each dot is an independent experiment and corresponds to the mean
999 of the counting of 10 fields, with around 70 cells counted, *i.e.,* around 700 cells per dot. n = 4
1000 to 10 independent experiments. Since sEVs used in infection assays were prepared each
1001 time in parallel between non-infected or hCMV-infected cytotrophoblasts from a given
1002 batch, statistical analysis was done by pairing the results between sEV NI and sEV hCMV for
1003 each independent experiment. ns, non-significant; *, $p < 0.05$; *** $p < 0.001$ by paired *t*-test.
1004
1005 **Figure 6: Effect of placental sEVs on neural stem cells permissiveness for hCMV.**
1006 NSCs were incubated with sEVs prepared from cytotrophoblasts (A) or *ex vivo* first trimester
1007 placental histoculture (B), which were either non-infected (sEV NI) or hCMV-infected (sEV
1008 hCMV). 200 sEVs per cell were used. NSCs were then infected by hCMV at a MOI of 3,
1009 simultaneously, 2 h, of 24 h after sEV incubation. 24 h later, expression of IE antigen was
1010 assessed by immunofluorescence. Quantification of the percentage of IE positive cells was
1011 carried out and normalized by the percentage of infection of cells infected by hCMV without
1012 any sEV (NT). Each dot is an independent experiment and corresponds to the mean of the
1013 counting of 10 fields, with around 70 cells counted, *i.e.* around 700 cells per dot. n = 4 to 7

1014 independent experiments. Since sEVs used in functional assays were prepared each time in
1015 parallel between non-infected or hCMV-infected cytotrophoblasts or placental explants from
1016 a given batch, statistical analysis was done by pairing the results between sEV NI and sEV
1017 hCMV for each independent experiment. ns, non-significant; *, $p < 0.05$ by paired *t*-test.
1018
1019 **Figure 7: Effect of sEVs prepared from amniotic fluid of naturally infected pregnant women**
1020 **on neural stem cells permissiveness for hCMV.**
1021 NSCs were incubated with sEVs prepared from amniotic fluid (AF) from patient NP19 (non-
1022 infected), NP6 (hCMV infected, AF negative for hCMV) or NP12 (hCMV infected, AF positive
1023 for hCMV). 200 sEVs per cell were used. NSCs were then infected by hCMV at a MOI of 3,
1024 simultaneously, 2 h, of 24 h after sEVs incubation. 24 h later, expression of IE antigen was
1025 assessed by immunofluorescence. Quantification of the percentage of IE-positive cells was
1026 carried out. Each dot is a biologic replicate and corresponds to the mean of the counting of
1027 10 fields, with around 70 cells counted, *i.e.,* around 700 cells per dot. n = 3 to 4 independent
1028 experiments. Results of ordinary one-way ANOVA test performed for the 3 different
1029 durations of sEVs incubation are the following: $p = 0.0374$ (*) for Simultaneously; $p = 0.0006$
1030 (***) for 2 h before; $p = 0.6415$ (non-significant) for 24 h before. Histograms represents the
1031 mean ± SEM of the percentage of infected cells in each condition. Statistical comparison
1032 between the conditions were done by unpaired *t*-test. ns, non-significant; *, $p < 0.05$; ** $p <$
1033 0.005.

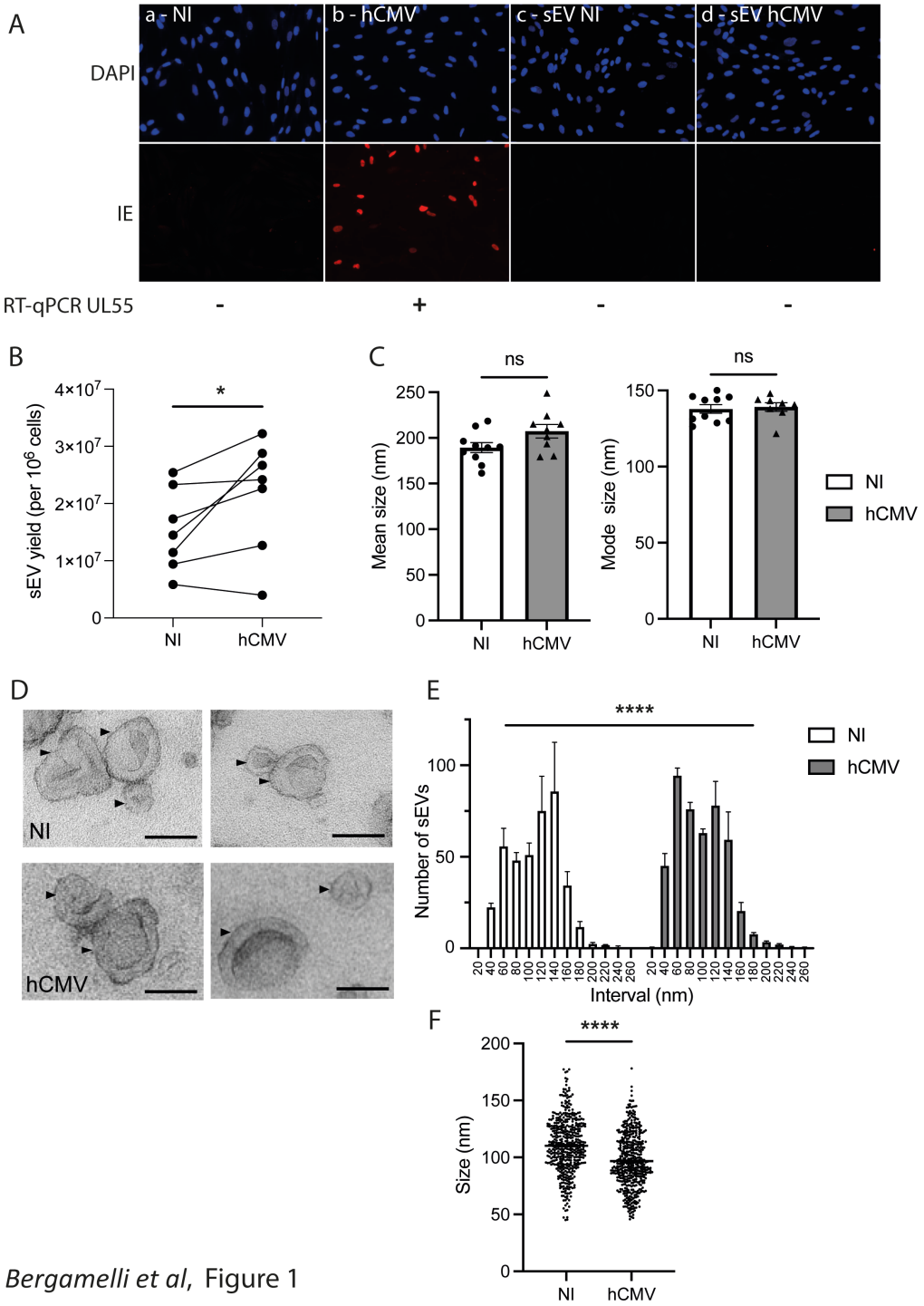

Bergamelli et al, Figure 1

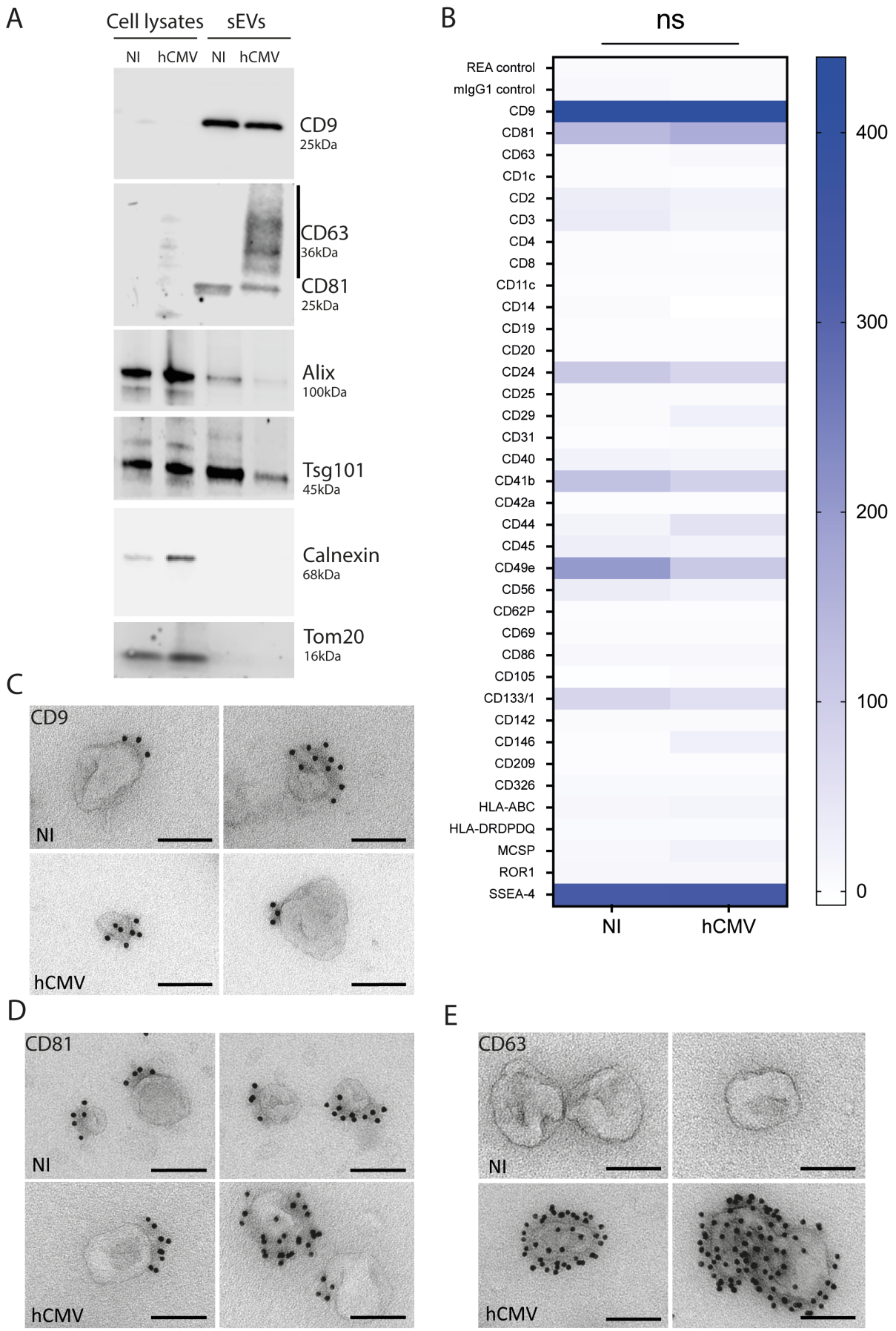

Bergamelli et al, Figure 2

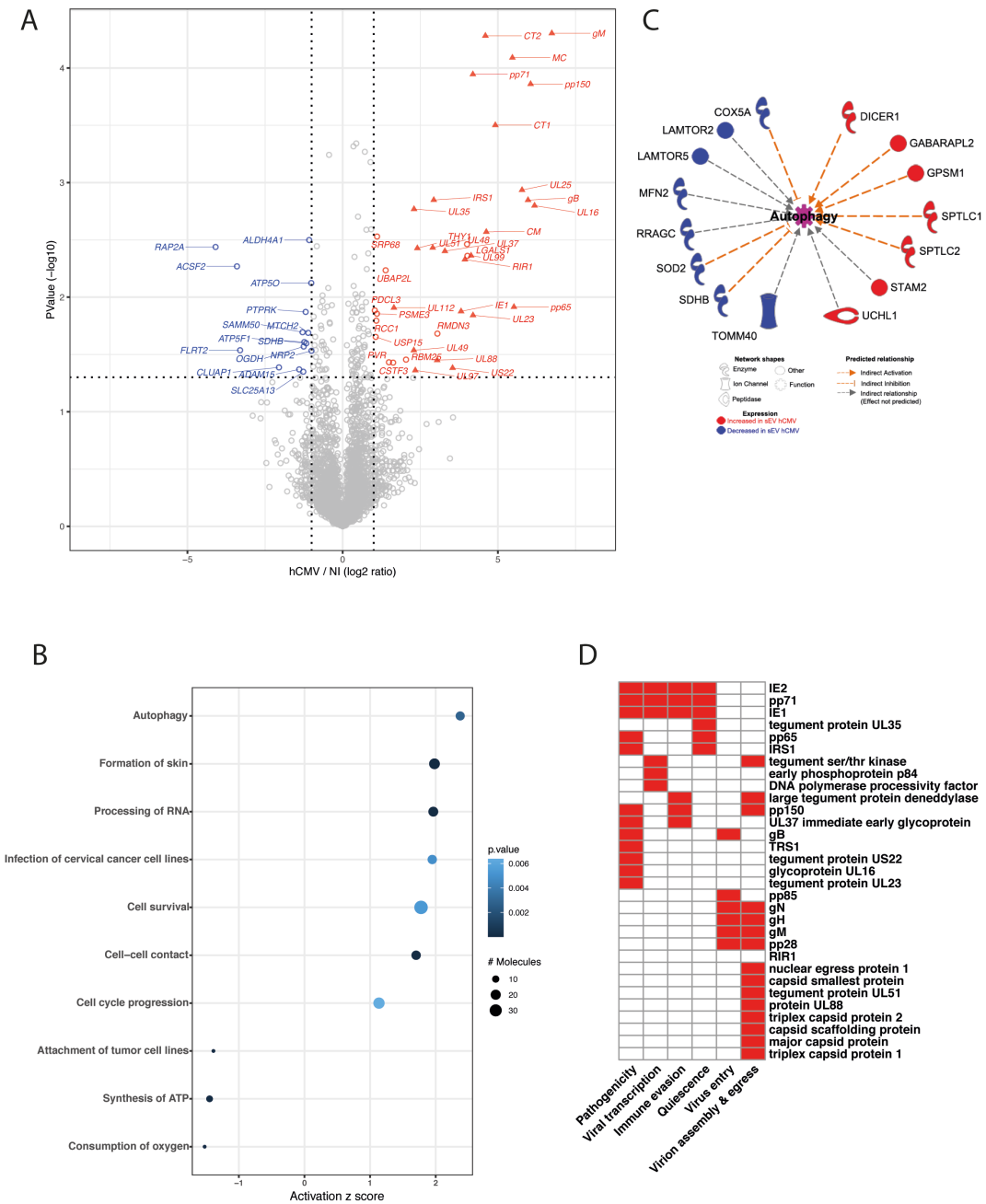

Bergamelli et al, Figure 3

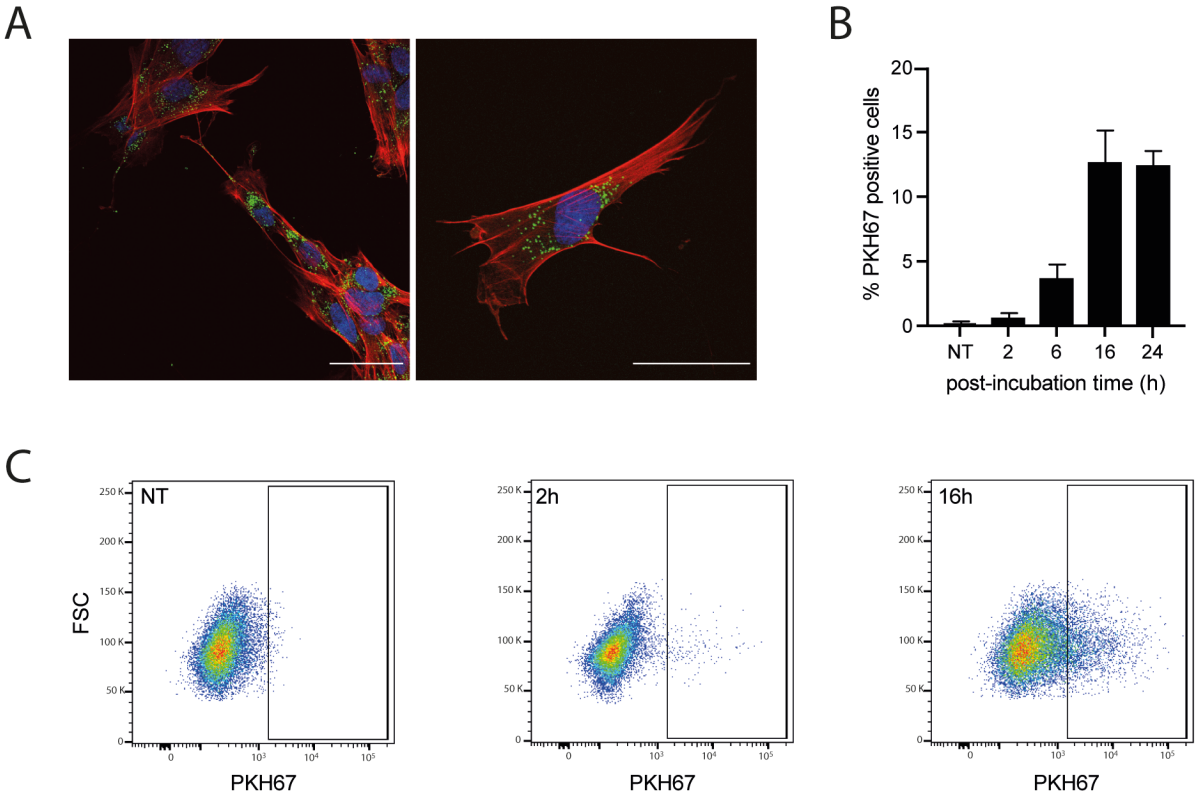

Bergamelli et al, Figure 4

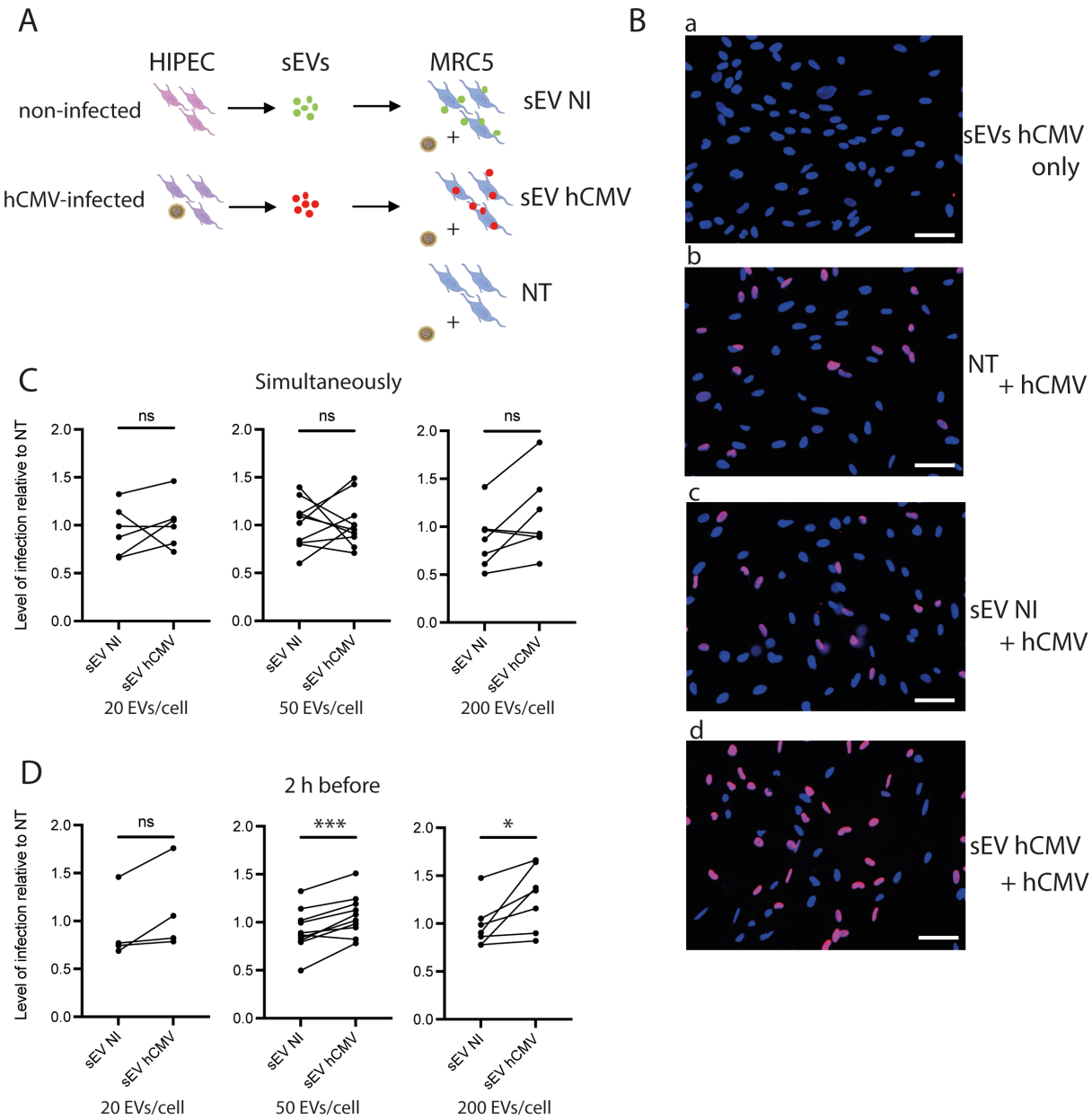

Bergamelli et al, Figure 5

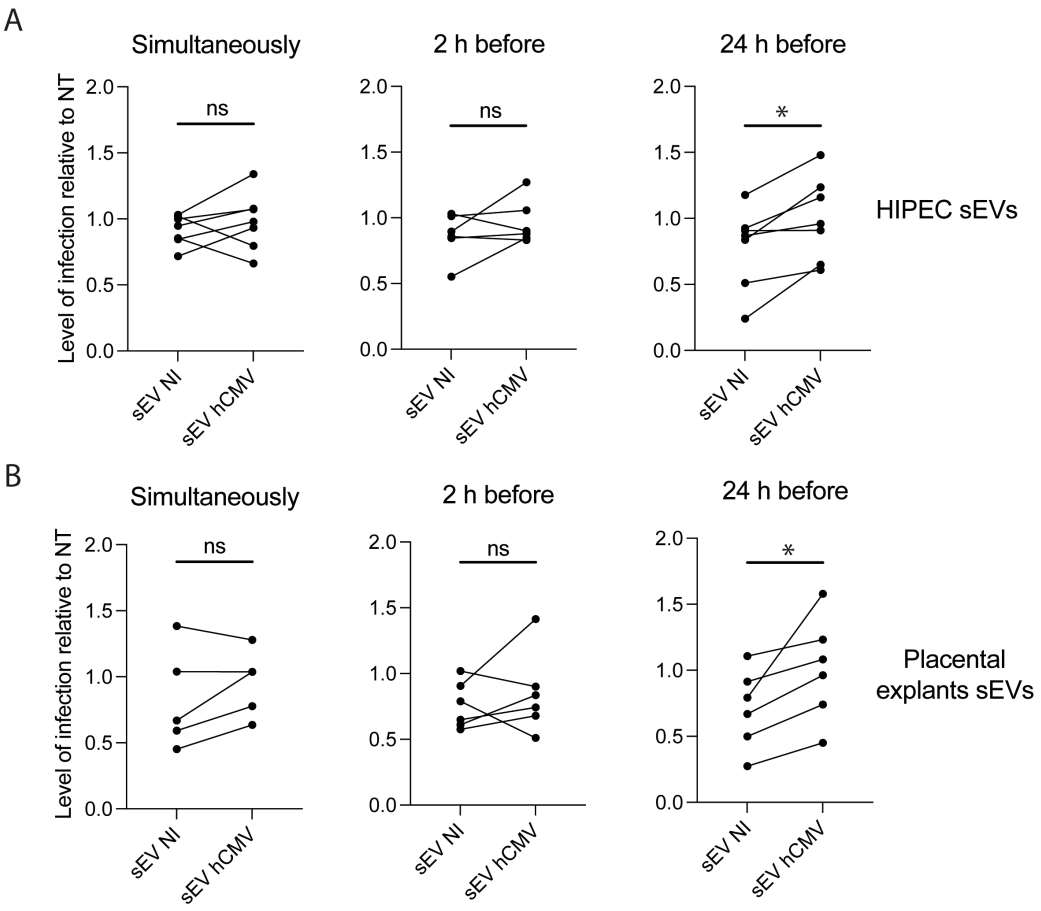

Bergamelli et al, Figure 6

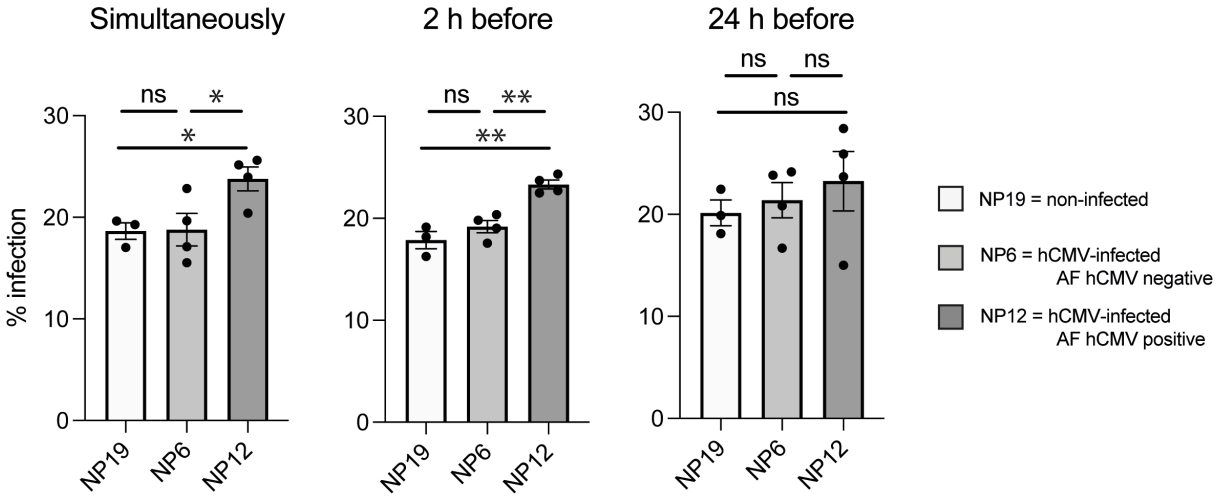

Bergamelli et al, Figure 7